Nuclear Engineering and Design 241 (2011) 3658–3677

Contents lists available at ScienceDirect

Nuclear Engineering and Design

journal homepage: www.elsevier.com/locate/nucengdes

Review

A review on the clad failure studies

Tanweer Alam[a], Mohd. Kaleem Khan[a,*], Manabendra Pathak[a], K. Ravi[b], Ritu Singh[b], S.K. Gupta[b]

[a] Department of Mechanical Engineering, Indian Institute of Technology Patna, Patliputra Colony, Patna, Bihar 800 013, India
[b] Atomic Energy Regulatory Board, Mumbai, India

ARTICLE INFO

Article history:
Received 26 June 2011
Received in revised form 29 July 2011
Accepted 3 August 2011

ABSTRACT

In this paper, an attempt has been made to systematically organize the research investigations conducted on clad tube failure, so far. Before presenting the review on the clad failure studies, an introduction to different clad materials has been added, in which the effect of alloying elements on the material properties have been presented. The literature on clad failure has been broadly categorized under the headings LOCA and RIA. The failure mechanisms like creep, corrosion and pellet–clad interaction have been discussed in details. Each subsection of the review has been provided with summary table, in which the studies are arranged in the chronological order. A small section on acceptance criteria for ECCS has also been included. The last section of the review has been dedicated to the core-degradation phenomena.

Contents

1. Introduction

Clad tubes or claddings or sheaths are the hollow cylindrical tubes used to provide an air-tight enclosure for the radioactive nuclear fuel such that the heat produced due to fission can safely be transferred to the coolant without contamination. The materials used for the clad tube fabrication are the zirconium based alloys due to their favourable properties like lower cross-sectional area to absorb the thermal neutron and resistance against corrosion at high temperature. A clad tube may have different sizes depending on the type of reactor. A typical clad tube has been shown in Fig. 1. Total volume of clad is not completely covered by fuel elements but a free space is available at ends for released fission product

Abbreviations: BCC, body-centered cubic structure; BDBA, beyond design basis accident; BWR, boiling water reactor; CHF, critical heat flux; DNB, departure from nucleate boiling; ECCS, emergency core cooling system; GWD, giga Watt per day; HCP, hexagonal closed packed structure; HR, heating rate; ID, inner diameter; IOP, internal over pressure; IP, internal pressure; LMP, Larsen Miller parameter; LOCA, loss of coolant accident; LWR, light water reactors; MTU, mega ton unit; NRC, nuclear regulatory commission; OD, outer diameter; PCMI, pellet–clad mechanical interaction; PHWR, pressurized heavy water reactor; PWR, pressurized water reactor; RBMK, Reaktor Bolshoy Moshchnosti Kanalniy (high power channel-type reactor); RIA, reactivity initiated accidents; RXA, re-crystallization annealed; SRA, stress relieved annealed; TCE, total circumferential elongation; VVER, Vodo-Vodyanoi Energetichesky Reactor(water–water energetic reactor).

* Corresponding author. Tel.: +91 612 2552019; fax: +91 612 2277383.
E-mail addresses: mkkhan@iitp.ac.in, kalimdme@gmail.com (Mohd.K. Khan).

0029-5493/$ – see front matter © 2011 Elsevier B.V. All rights reserved.
doi:10.1016/j.nucengdes.2011.08.009

Nomenclature

Symbols

A	Arrhenius constant
k	gas constant
O_x	oxygen uptake
P	pressure (MPa)
Q	activation energy
T	temperature (K)
$\dot{T}$	heating rate (K/s)
t	time (s)
w	zirconium metal weight reacted (mg/cm^2)

Greek letters

σ	stress
ε	strain
$\dot{\varepsilon}$	creep rate
α	alpha phase
β	beta phase

Subscript

e	effective
f	failure
i	initial
l	logarithmic
θ	circumferential direction
θB	burst hoop
θt	tensile hoop
ss	steady state

Superscript

n	exponent

gases. Springs at ends are used to keep the fuel elements intact with insulator Al_2O_3 between them and the spring (Cacuci, 2010).

The claddings have thin walls with thickness ranging from 0.4 to 0.8 mm, and their life is of 2–4 years for CANDU reactors (Krishnan and Asundi, 1981). As a matter of fact that clad tube is never used 'single' in an operational reactor. The particular arrangement, shown in Fig. 2, is meant for CANDU type reactors, where a number of clad tubes containing fuel pellets are held together to form a fuel bundle. A fuel bundle comprises either 19 or 37 clad tubes depending on the capacity of the nuclear power plant. Clad tubes in a fuel bundle are separated from each other with the help of spacer grids. These fuel bundles are placed inside the pressurized tubes through which coolant flows. Calandria tube provides a cover to the pressurized tube with annulus region filled with carbon dioxide gas.

Due to their proximity to fuel, the clad tubes are the first to fail in an accident scenario. The accidents can be broadly classified as: (1) loss-of-coolant accident (LOCA) and (2) reactivity-initiated accident (RIA). In LOCA, the coolant supply is affected and the heat produced during the fission could not escape, resulting in a sudden rise in temperature and pressure inside zircaloy clad tubes. The tube starts to swell and finally bursts. Consequently, clads are subjected to the damage mechanisms like creep, loss of ductility and corrosion. In RIA, there is an unwanted increase in fission rate and an abrupt rise in reactor power leading to the damage of reactor core. The damage mechanisms pellet–clad mechanical interaction (PCMI) and departure from nucleate boiling (DNB) characterize the RIA (OECD Reports, NEA Nos. 6846 and 6847, 2010).

The failure studies play vital role in improving the safety criteria of the reactor core of the nuclear power plants. A lot of research work, mostly experimental, pertaining to clad material development and its failure has been reported in the literature since last five decades. Numerous review articles are also available on clad tube behavior during steady as well as transient conditions (Kass, 1964; Mishima et al., 1966; Pickman, 1972, 1994; Maki and Ooyama,

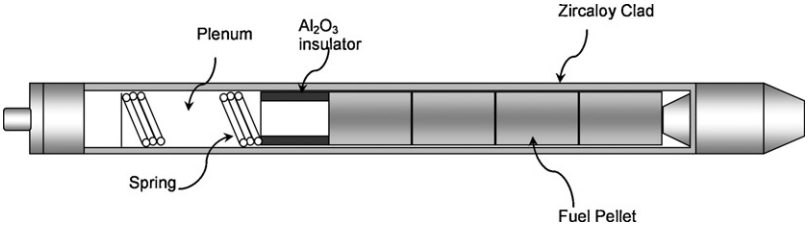

Fig. 1. Sectional view of clad tube (Cacuci, 2010).

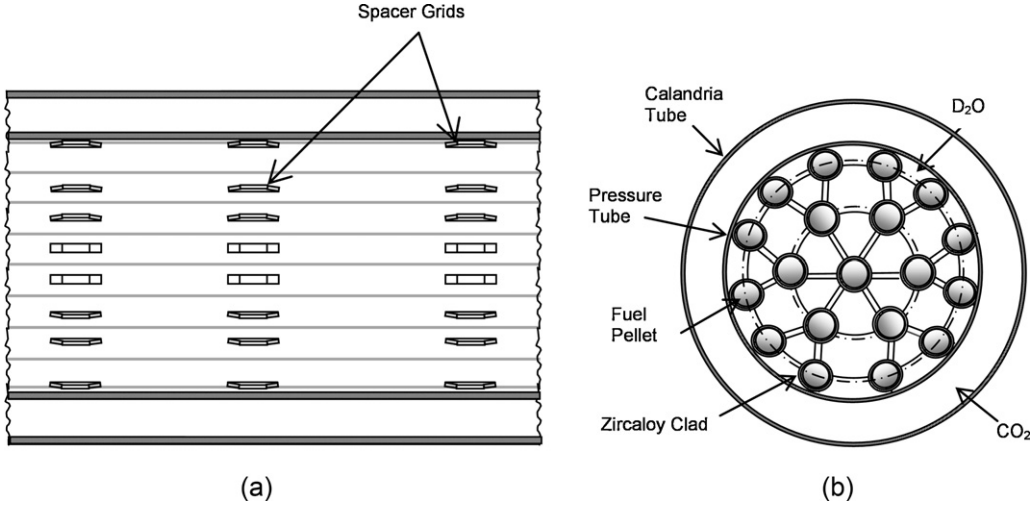

Fig. 2. Clad and fuel bundle arrangement used in CANDU reactors (a) front view, (b) side view.

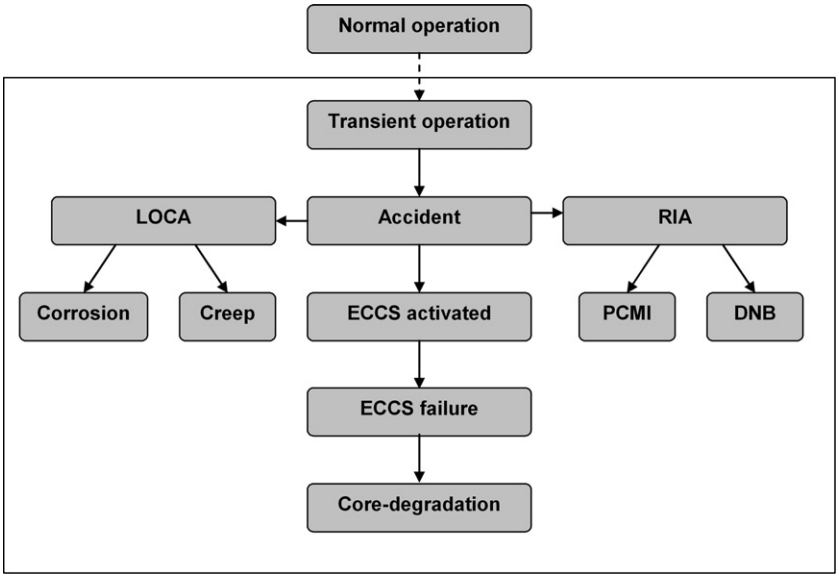

Fig. 3. Sequence of events in accident scenario in a nuclear power plant.

1976; Furuta et al., 1978; Krishnan and Asundi, 1981; Burman et al., 1984; Erbacher and Leistikow, 1987; Garzarolli et al., 1996; Cox, 2005; Sabol, 2005; Foster et al., 2008; Lewis et al., 2009).

These articles have been discussed in details under different headings later. None of these articles presented a comprehensive review. An attempt to compile the work related to clad failure at one place has not been made so far. Therefore, there is a need to have a comprehensive review of the clad failure studies. The present paper not only summarizes important studies but also reviews meticulously the developments in clad material and its failure during LOCA and RIA conditions. The focus of the present review is precisely on the transient behavior of the zircaloy clad leading to accident (LOCA/RIA). However, for the sake of better understanding the clad tube behavior under steady or normal has also been discussed in parallel at some places. Fig. 3 has been drawn to give readers an insight into sequence of events in a nuclear power plant in an accident scenario. As soon as the abnormal activity in the reactor of the plant is detected, which may be due to LOCA or RIA, the emergency core cooling system is activated. In the worst case scenario, if this system fails to control the reaction, the core-degradation starts with the bursting of clad tubes, pressure tube or even calandria tubes. In such a case, a complete core meltdown is imminent. The same figure also represents the sequence of our review paper after the discussion on clad materials.

The thorough review has been presented systematically in tabular form in the chronological order under each section.

2. Materials for clad tubes

This section is dedicated to clad tube materials and their development. This section has begun with zirconium based alloys and the influence of alloying elements on material properties. After that a historical development of clad material along with some of the important studies has been discussed.

Clad tubes are the vital part of a nuclear reactor as they not only provide an enclosure to the highly radioactive fuel but also remain in direct contact with the coolant during reactor operation which makes it vulnerable to corrosion. Its integrity becomes very important during accidental scenario when most of the heat emitted due to fission reaction accumulated inside the clad tubes. Hence, the material used for clad tubes must have important characteristics like low cross sectional area to absorb thermal neutrons, high thermal conductivity, high strength, high resistance against corrosion and high dimensional stability.

To get additional properties for better operation in water cooled reactors zirconium was alloyed with constituents like tin, iron, chromium, nickel, and niobium, Table 1 shows composition of various zirconium alloys used as clad materials. Tin a major constituent

Table 1
Composition[a] (weight %) of various zirconium alloys.

Alloys	Tin	Iron	Chromium	Nickel	Niobium	Remarks
Zircaloy-1	2.50	–	–	–	–	Not suitable for reactor operation
Zircaloy-2	1.50	0.12	0.10	0.05	–	Although it is used in BWRs but several cases of clad failure have been reported in the literature due to localized corrosion (Shimada et al., 2005)
Zircaloy-3A	0.25	0.25	–	–	–	Lowering tin content improves corrosion resistance but reduces creep resistance and yield strength
Zircaloy-3B	0.50	0.40	–	–	–	
Zircaloy-3C	0.50	0.20	–	0.20	–	
Zircaloy-4	1.50	0.20	0.10	–	–	Recommended for PWR
ZIRLO	1.02	0.10	–	–	1.01	Recommended for PWR for high burn-up fuels
M5®	–	0.05	0.015	–	1.0	Better corrosion resistance than zircaloy-4 at higher temperature
É110	–	–	–	–	0.95–1.05	Recommended for PWR, RBMK and VVER applications
É125	–	–	–	–	2.20–2.60	
É635	1.1–1.3	0.3–0.4	–	–	0.95–1.05	
OPT ZIRLO	0.66	0.11	–	–	1.04	Suitable for higher corrosion condition and have sufficient in reactor creep resistance
X5A (AXIOM)	0.5	0.35	0.25		0.3	Better in-PWR properties in comparison to ZIRLO at high burn-up

[a] Remainder zirconium.

Table 2
History of clad material development.

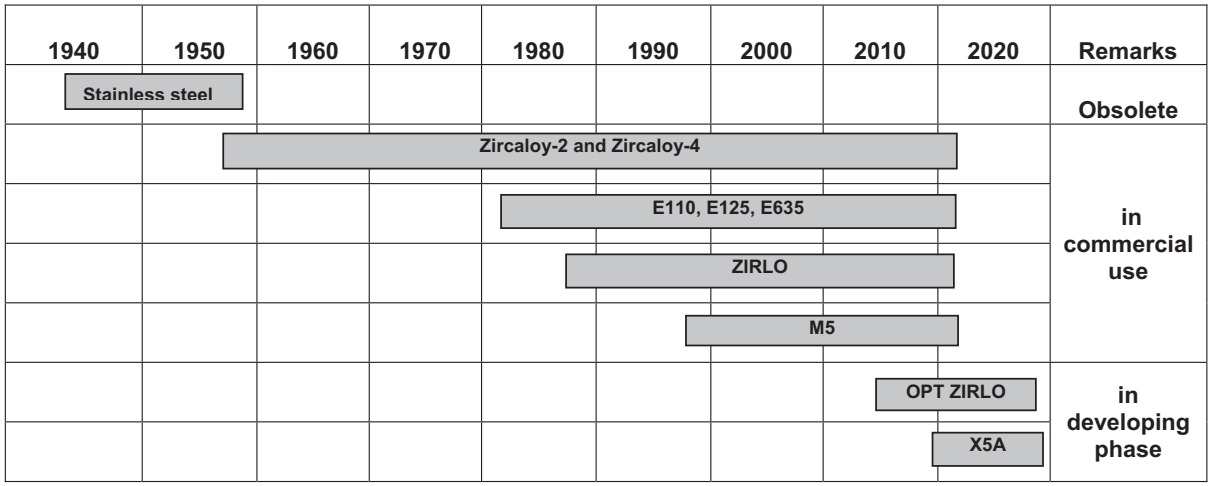

reduces the effect of nitrogen, which enhances the corrosion of zirconium in high temperature water. Nickel, chromium and iron also decrease the corrosion of alloy in steam as well as in high temperature water. Chromium not only increases the corrosion resistance but also the hardness of element while nickel enhances the hydriding effect so their amount is kept within the permissible limit. The sum of iron, chromium and nickel must fall between 0.18 and 0.38% (Kass, 1964). Later on, addition of niobium to zirconium provides higher strength to the alloy and makes its suitable for high burn up fuels. From the review of literature, zirconium alloys for reactors may be thought to have two broad categories: Zr–Sn and Zr–Sn–Nb compositions.

As said earlier, most of the clad failure studies have been done with zircaloy-2 or zircaloy-4 as the tube material, where the main alloying elements are zirconium and tin. The phase diagram of Zr–Sn has been shown in Fig. 4. The band in which zircaloy-2 and zircaloy-4 lie has also been shown as shaded region in the figure. Unalloyed zirconium has two distinct type of crystal structure, hexagonal close-packed (HCP) in α-phase up to 850 °C. From the temperature of 950 °C to its melting point 1845 °C, there exists body-centered cubic (BCC) β-phase. Further, there exists a mixed-phase or transition phase (α + β) in the temperature range of 850–950 °C. During steady state or normal plant operation, the maximum service temperature of zircaloy clad surface is 400 °C (Azevedo, 2011), which means zircaloy material remains in α-phase (HCP). On the other hand, during transient condition leading to accident, the overheating causes the clad surface temperature to rise and change of phase takes place, i.e. from α-phase to mixed or transition (α + β)-phase and then from (α + β)-phase to β-phase (BCC). The HCP structure is anisotropic whereas BCC structure is isotropic in nature. Obviously, the three phases have altogether different properties. Thus, the rate of creep (deformation) and the rate of corrosion (oxidation) vary from phase-to-phase. The detailed description on the effects of these parameters on clad tube failure has been covered in the subsequent sections.

Table 2 gives a glimpse of the history of clad material development. Earlier in 1950s, stainless steel was used as clad tube for fuel elements but due to its corrosive nature at higher temperature, the focus was shifted towards the development of zirconium alloys (Mishima et al., 1966). Zirconium having all the above properties was not in use during early stage of reactor development due to high extracting cost from its parent metal zircon containing hafnium having 600 times larger thermal absorbing cross sectional area than zirconium. Zirconium extraction was done with the invention of less expensive Kroll process, developed by W.J. Kroll (Kass, 1964).

Table 3 depicts some of the important studies on the development of clad material. Kass (1964) reviewed the work on the development of zirconium alloys viz., zircaloy-1, zircaloy-2, zircaloy-3 and zircaloy-4 with a special focus on corrosion prop-

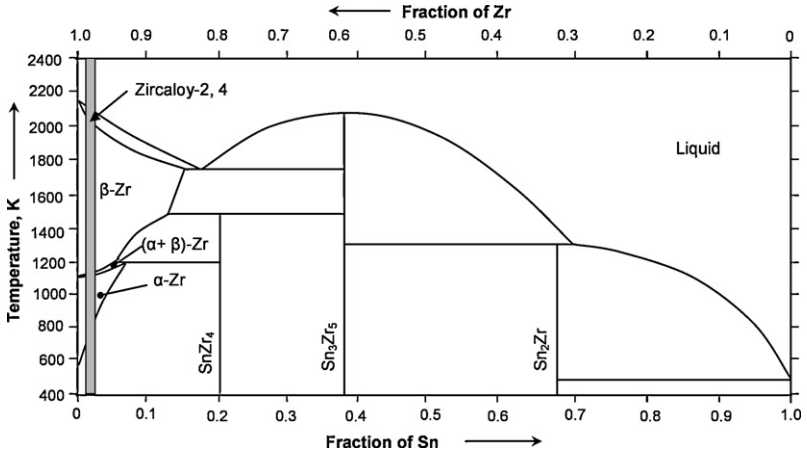

Fig. 4. Zr–Sn phase diagram (Dupin et al., 1999).

Table 3
Investigations on the development of clad material.

Authors (year)	Aspect	Remarks
Kass (1964)	Zircaloy development	• Tin is the major component for enhancing the corrosion resistance • Nickel free zircaloy-4 has less affinity of absorbing hydrogen at high temperature and pressure environment
Lustman (1979)	Zirconium technology development from 1955 to 1975 (review)	• The paper discusses the evolution of Zr–Sn and Zr–Nb based zirconium alloys as viable material for clad
Krishnan and Asundi (1981)	Zircaloy application	• In the absence of oxygenated boiling condition zircaloy-2 is suitable as structural material
Sabol et al. (1989)	Cladding alloy for high burnup fuel	• Sn–Nb–Fe alloy had higher corrosion resistance, better up to 50%, than zircaloy-4 at the highest burnup
Nikulina (2004)	Zirconium alloys development	• E110 and E635 and their modified versions E110M and E635M have been discussed in details
Sabol (2005)	ZIRLO™ development	• Niobium addition enhanced the corrosion resistance, irradiation growth, and creep properties of zircaloy clad for high burn-up fuels
Foster et al. (2008)	OPT ZIRLO properties	• Change in ZIRLO microstructure would enhanced the creep strength Final tube area reduction has an impact on creep strength
Garde et al. (2010)	Advanced Zirconium base alloys (AXIOM)	• X5A has comparable corrosion resistance, lower fuel rod growth and better weld corrosion resistance in comparison to ZIRLO
Mardon et al. (2010)	M5® a breakthrough in Zr alloy	
Steinbrück and Böttcher (2011)	M5® and ZIRLO™ Comparison with zircaloy-4	• After the transition up to accelerated kinetics M5® showed the lowest long-term oxidation kinetics up to 1300 K

erties of zircaloy-2 and zircaloy-4 in high temperature water and steam environment. The composition of the alloys has been shown in Table 1. The following observations can be made from this study:

- Zircaloy-2 and zircaloy-4 are preferred over zircaloy-1 and zircaloy-3 due to their better strength and corrosion resistance.
- Zircaloy-2 is best suited for BWR conditions where pressure and temperature is comparatively lower than PWR. On the other hand, the use of zircaloy-2 was not recommended in PWR due to the formation of hydride at high temperature and pressure.
- For application in PWR, zircaloy-4, obtained by removing nickel and increasing iron percentage from 0.12 to 0.2, is recommended. In zircaloy-4, the hydride formation is decreased due to the removal of nickel and corrosion resistance is further increased due to increased iron percentage.
- The reduction of Sn, as in case of zircaloy-3 or in general, increases the corrosion resistance but decreases the yield stress and creep resistance, two important characteristics exhibiting the integrity of clad tubes.

Lustman (1979) presented an evolution in the zirconium technology for the period 1955–1975. It was found by comparison that Zr–Sn based zircaloys and Zr–Nb compositions were viable materials.

Krishnan and Asundi (1981) described the historical development of zirconium and its alloys for nuclear reactors. Their reviewed work was similar to that of Kass (1964). In addition, they focused on the alloying of zirconium with niobium. They discussed the suitability of clad tubes of such material in high temperature conditions and the result was higher strength and higher corrosion resistance.

In order to reduce the radioactive wastes and for efficient utilization of nuclear fuel in reactor fuel burn-up is increasing. Hence, newer and traditional clad tube material used for this high burn-up fuel should comply with their mechanical behavior. In high burn-up fuels, the coolant temperature is very high. For these conditions, zircaloy clad tubes developed earlier have not been found suitable because of their low corrosion resistance at higher temperature. In such places, clad tubes should be made of a material that would give a solution to mechanical, chemical, and metallurgical problems. To overcome these problems, recently different alloys of zirconium and niobium like ZIRLO™ and M5®, termed as advanced cladding alloys, have been developed to get a replacement for zircaloy-4 in PWR applications. To overcome these problems, recently an alloy known as ZIRLO has been developed. Sabol et al. (1989) developed advanced zircaloy cladding with niobium as an alloying element. The clad made up of this material was subjected to long term out-of-pile autoclave corrosion test and high burn-up irradiation test in PWR environment. Lower corrosion rates were observed in the developed alloy as compared to that in zircaloy-4. ZIRLO alloy (contains 1% Nb) showed a lower in-reactor creep and rod growth as compared to zircaloy-4. Further, Sabol (2005) has made a comparative study of zircaloy-4 and ZIRLO for PWR application. Effect on the properties of zircaloy with different composition of niobium with zirconium has been discussed. It has been found that not only among all zirconium–niobium alloys but also in comparison to zircaloy-4, ZIRLO has better corrosion resistance, irradiation growth, and creep properties for high burn-up fuels. ZIRLO is found to have a better dimensional stability than zircaloy-4 and thus, make it suitable for high temperature applications.

Recently, another material named OPT ZIRLO (optimized ZIRLO) has been developed and is found to have superior properties than ZIRLO. Foster et al. (2008) have compared the new material for clad, i.e., OPT ZIRLO with standard ZIRLO. It has been found that OPT ZIRLO having lesser amount of tin (0.6–0.8%) in comparison to ZIRLO (1%) has higher corrosion resistance. The decrease in in-reactor creep strength of OPT ZIRLO from STD ZIRLO due to lower tin content has been compensated by fabrication changes like final tube area reduction and final annealing temperature.

Several authors have made a comparison of M5, with zircaloy-4. It has been established that M5 is a better choice than zircaloy-4, when subjected to severe thermomechanical loading and has higher corrosion resistance. Addition of oxygen along with niobium made it different from ZIRLO (Mardon et al., 2000, 2010; Elbachiri et al., 2008; Stern et al., 2008).

Nikulina (2004) presented the results of studies of zirconium alloys É110 and É635 used in VVÉR-1000 reactors. The influence of the composition on the properties of alloys É110 and É635 was studied and modifications (É110M and É635M) were suggested. It was observed that É110 had a high corrosion resistance in water at high pressure and temperature. Also it corroded intensely in boiling water medium in the presence of lithium. É635, on the other hand, was found to have good corrosion resistance in boiling water whereas low corrosion resistance in water under pressure. Both these alloys had been found to have high strength, creep resistance, and resistance to radiation growth. Asmolov et al. (2002) presented the detailed LOCA related ductility of É110.

Most recently, advanced zirconium alloys, designated collectively as AXIOM™ for PWR applications have been developed. Garde et al. (2010) have conducted a review on X5A alloy of AXIOM™. Following points have to be remembered:

- Corrosion resistance of low temperature processing X5A (LTP-X5A) is 30% lower than that of ZIRLO through a burn-up of 50GWd/MTU, whereas high temperature processing X5A (HTP-X5A) has comparable corrosion resistance to that of ZIRLO.
- Fuel rod growth of LTP-X5A is lower than that of ZIRLO whereas in case HTP-X5A, it is comparable to ZIRLO.
- Hydrogen pick-up of HTP-X5A is about 35% lower than that of ZIRLO.
- For burn-ups about 50GWd/MTU, X5A is a promising alloy for PWR application.

Steinbrück and Böttcher (2011) have compared M5, ZIRLO and zircaloy-4. Prior to transition phase same oxidation kinetics has been observed for all three alloys, while after the transition up to accelerated kinetics M5 showed the lowest long-term oxidation kinetics up to 1300 K. This study has been conducted in air (oxidation) environment and hence is not very relevant to in-reactor cases.

3. Clad failure studies

The volumes of papers on the experimental investigations on the clad tubes have been published. However, the present work will focus only on the failure studies on zircaloy clad tubes especially during transient condition leading to accident. The degradation of clad tubes occurs during normal plant operation as well. It occurs mainly due three reasons (a) waterside corrosion, (b) hydriding and (c) radiation damage. Due to continuous contact of water, corrosion of clad causes the formation of oxide layer on it. This oxide layer is more or less uniform for PWR. Hydriding occurs due to absorption of hydrogen on the clad surface, which results in lower ductility. However, the traces of hydride are also available in the bulk as well. Radiation damage also reduces the life of clad tube (OECD report NEA No. 6846, 2010).

Therefore, it should be remembered that the clad tube failure occurs due to its degradation because of corrosion during normal operation in addition to accelerated rate of corrosion and plastic deformation during transient condition leading to accidents. During normal operating condition, change in the clad properties is not very significant. On the other hand, during transient condition leading to accident, a remarkable change in clad properties is observed due the change in microstructure.

Here in this paper, the performance behavior of zircaloy clad tubes has been studied for both type of accidents, i.e. LOCA and RIA. The operating parameters range like heating rate, internal pressure, pressurizing medium, exposure time and the environment surroundings the clad on diametral expansion (ballooning), rupture characteristics and bursting of the clad tube has been presented in summary tables. The results of these studies are used to formulate the acceptance criteria for emergency core cooling system (ECCS), a system activated in the accident scenario.

As discussed earlier in Section 1 in the description of Fig. 3, the review of experimental investigations on failure studies has been divided in the following manner:

- LOCA
  - Corrosion
  - Creep
- RIA
  - Pellet–clad mechanical interaction (PCMI)
  - Departure from nucleate boiling (DNB)

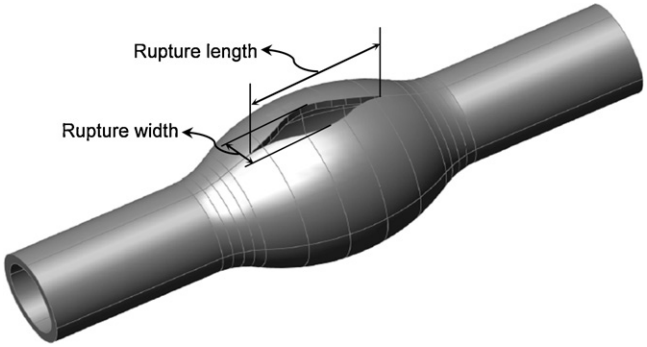

Fig. 5. Schematic diagram of a typical ruptured clad tube.

- Criteria for ECCS
- Core degradation phenomena

3.1. Loss-of-coolant accident (LOCA)

The loss of coolant accident, popularly known as LOCA, is an accident scenario when there is a scarcity of coolant in the reactor circuit. There are two mechanisms of clad tube failure due to LOCA, viz. corrosion (oxidation) and creep (deformation). The two mechanisms go in parallel until the tube bursts. As discussed in the previous section, during normal operation, the oxide layer on the clad tube surface forms slowly and uniformly. At the oxide layer-tube interface the zircaloy is in α-phase with the fine dispersion of second phase. During LOCA, the overheating leads to continuous rise in temperature. As soon as the temperature reaches 800 °C the α-phase starts transforming to β-phase. Simultaneously, the oxidation reaction begins to accelerate and as such the layer thickening takes place. The oxygen dissolved on clad surface, which stabilizes α-phase. Below this high oxygen layer of α-phase, there lies a layer of β-phase and above it is the oxidized layer. Oxygen dissolution causes embrittlement of the layer of α-phase. If this brittle layer is allowed to grow, it will severely hurt the tube's structural integrity. Therefore, there is a need to curb the growth of the outer brittle oxide layer and middle oxygen rich α-phase layer and the thinning of load bearing inner β-phase layer must be avoided during quench phase of LOCA. The quenching introduces a number of thermal stresses on the already weakened oxidized clad tube surface.

As a result of loss of coolant pressure outside the clad falls and a rise internal pressure due to overheating causes plastic deformation which leads to ballooning and burst. A typical ruptured-clad tube has been shown by means of schematic diagram in Fig. 5. The ballooning may affect cooling of the fuel assemblies whereas the burst will cause oxidation at the inside tube surface. The hydrogen released due to oxidation during normal and transient operation, i.e. during LOCA, is absorbed by the clad tube surface leading to its embrittlement. The quenching during ECCS further intensifies the embrittlement. The heat released in the oxidation reaction cannot be dissipated by quenching and as such run-away or auto-catalytic oxidation occurs, which finally contributes to core melting (Erbacher and Leistikow, 1987; and OECD report NEA No. 6846, 2010).

The following three phenomena need to be explained to describe LOCA:

Deterioration of heat transfer mechanism

The heat transfer is badly affected due to the loss of coolant in the reactor. The coolant is in direct contact with the fuel bundles and due to the loss, less coolant will be available for taking away the heat generated inside the clads. This deterioration of heat transfer

mechanism causes the increase in level of decay heat and reactor trip system comes into action.

Decay heat

It is the heat released due to decay of radioactive nuclides produced during the fission reaction. The accurate determination of decay heat released from nuclear fuel cycle is helpful in activating the reactor trip system and is a measure of safety assessment of a nuclear power plant (Tobais, 1980).

Reactor trip

As soon as the LOCA is detected, the reactor trip mechanism is automatically activated after receiving the abnormal signals due to decay heat. Reactor trip system is one of the important instrumentation and control system, installed within the pressurized vessel. Through this system, the control rods are moved into the reactor, which absorb neutrons and thus, slow down the nuclear fission reaction (Teichel and Pouget-Abadie, 1999). Although the reactor shutdown takes place but there is still heating of core due to stored energy and decay heat. It may cause deformation of clad tube with increase in temperature above 600 °C. Ballooning of clad tube due to increase in temperature may cause the blockage of coolant passage which is supplied due to action of emergency core cooling system (ECCS). Circumferential elongation of clad along with axial constraint may further cause the clad bursting in absence of sufficient cooling. The sudden supply of water, termed as re-flooding to cool the core, quenches the heated clad, which may further worsen the situation. As a result, the shattering of cladding disperses fuel fragments.

Here are some of the significant contributions on the clad tube failure due to LOCA have been presented here in this section. One such study was conducted by Mishima et al. (1966) way back in 1965 on clad tubes of stainless steel and zircaloy under LOCA conditions. Their work was focused on three aspects of clad failure:

(a) Effect of oxidation during heating up to bursting temperature in the steam environment (130 °C temperature and 3 atm pressure) on the tensile strength of fuel cladding material.
(b) Determination of bursting temperature of pressurized clad tube.
(c) Effect on previously corroded clad during the burst test.

It was observed that there was no appreciable effect on the effective thickness of clad tube either of stainless steel or zircaloy. No substantial thickening of cladding wall due to corrosion under normal operating conditions during the LOCA was observed.

Hardy et al. (1974) formulated the burst test procedure for closed-end zircaloy clad and suggested the use of the closed-end burst test for the characterization of biaxial mechanical properties of zircaloy clad tube. However, it should be remembered that the burst test is not used as NRC criteria test, instead tube compression test is used for that purpose. It was further suggested that the most desirable burst test apparatus was one which had low stored energy (internal pressure). Following were the results:

- The ultimate hoop strength increased with the increase in strain rate whereas the total circumferential elongation decreased with the increase in strain rate.
- Increase in the stored energy of the pressurizing system reduced the total circumferential elongation and increased the strain rate.
- The use of internal mandrel increased the total circumferential elongation. The use of mandrel was recommended as optional if the ratio of internal diameter to the diametral clearance of 20 ± 2.

The studies on corrosion and creep have been presented as the subsections of this section.

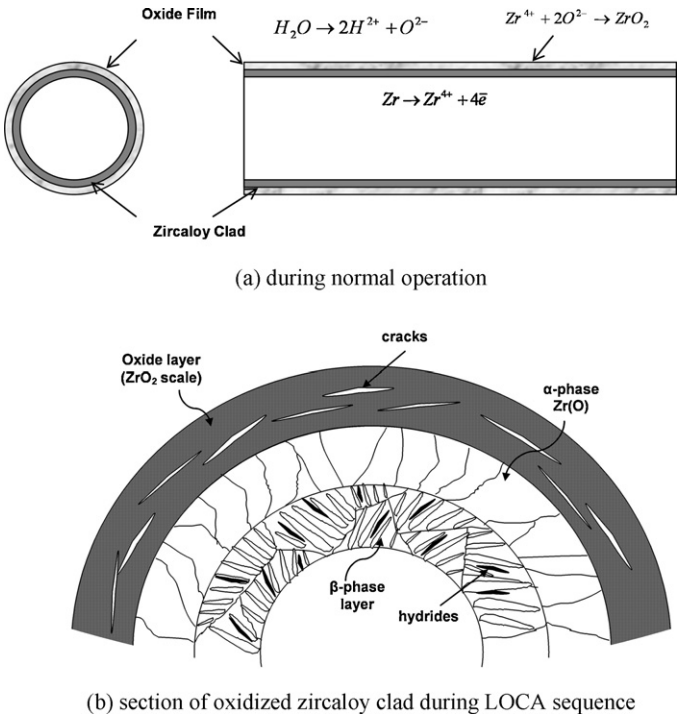

Fig. 6. Formation of oxide film on zircaloy clad (a) during normal operation, (b) section of oxidized zircaloy clad during LOCA sequence.

3.1.1. Corrosion

This section has been dedicated to the studies done on corrosion of clads and effect of hydrogen absorption on clad tube. Clad tube, throughout its life, in reactor remains in direct contact with the coolant which makes it susceptible to corrosion. Fig. 6 shows the mechanism of corrosion during normal operation and transient LOCA sequence. During normal operating condition, as explained earlier, clad tube oxidizes slowly in reactor water with the growth of thin oxide layer on the surface. During LOCA, sudden heat-up, cool down and quench caused the acute change in clad properties. The thickness of oxide layer during LOCA rises with clad tube oxidation. The brittle nature of oxide layer and newly formed, oxygen-rich α-phase layer, threatens to the integrity of clad tube, whereas the innermost β-layer, on the other hand, is the only load bearing layer which needs to protected from thinning. During normal operation and LOCA, hydrogen released during corrosion reaction is absorbed by the clad tube.

Table 4 shows a summary of studies on corrosion. The nascent clad in the reactor has thin layer of adherent black oxide film. This layer acts as protective cover for the clad. At high temperature in steam or water further oxidation of clad produces thick oxide film on the surface and with the passage of time degradation of oxide film caused its color change from black to white, a non-adherent oxide film, with crack formation, as shown in Fig. 6. The formation of oxide film reduces the conductivity of the clad. Also it is a known fact that thermal conductivity is temperature dependent property and any change in temperature would ultimately change the thermal conductivity. It has been seen that the thermal conductivity of oxide layer is also greatly influenced with the type of oxidation environment, viz. steam, air, vacuum and inert (Maki and Ooyama, 1976). It has been established that oxide scales induce growth stresses, which contribute significantly in the deformation of zircaloy clad under the influence of applied stress (internal operating pressure), especially when nitrogen is present in the oxidizing atmosphere (Erbacher and Leistikow, 1987).

Table 4
Studies on corrosion.

Authors (year)	Aspect	Clad tube outside and Inside environment		Remarks
		Outside environment	Inside environment	
Emmerich et al. (1969)	Clad tube failure during thermal excursion	Steam and argon	Helium	• Failure in inert environment was of ductile nature while brittle nature failure occurred in steam environment
Pickman (1972)	Zircaloy clad properties	Water and steam	–	• Zirconium hydride presence up to 200 ppm H_2 did not have any detrimental effect
Maki and Ooyama (1976)	Clad interaction with water and steam	Water and steam	Argon	• White oxide film thermal conductivity (K) value was lesser than black oxide film
Furuta et al. (1978)	Clad behavior during LOCA	Steam and vacuum	Argon	• Extent of ballooning was found within the 30 mm of ruptured region
Furuta and Motohashi (1980)	Surface product on zircaloy under LOCA conditions	Steam	Argon	• Layer of ZrO_2 was found on outside surface while on inside surface mixture of ZrO_2 and ZrO was observed
Hindle and Mann (1982)	Zircaloy clad deformation under convective cooling	Steam	–	• Convective or radiative cooling had no effect on clad diametral strain for same pressure–temperature • Deformation shape controlling in radial direction was found for convective cooling
Uetsuka et al. (1982)	Zircaloy clad embrittlement due to oxidation	Steam	–	• Clad ductility was found to decrease with weight gain due to oxide layer • Clad embrittlement occurred due to H_2 absorption on inside surface
Sagat et al. (1984)	Zircaloy clad failure in LOCA conditions	Steam and vacuum	Helium	• Ductility reduction due to oxidation for specified heating rate was observed for temperature above 1000 °C • CANDU clad failure was observed due to local overstrain or beryllium-assisted inter-granular cracking
Burman et al. (1984)	Fuel rod deformation in LOCA	Steam	–	• For LOCA ballooning and burst model heating rate, burst stress and burst temperature were taken as variables
Cox (1985)	Hydrogen absorption mechanism	Water and steam	–	• Hydrogen diffusion into alloy during corrosion occur for those species which are produced during corrosion reaction
Hofmann and Neitzel (1987)	Clad oxidation under SFD conditions	Steam	Argon + 25% vol of oxygen	• UO_2/Zr reaction occurred as rapidly as the steam/Zr
Pickman (1994)	Clad corrosion behavior	Water and steam	–	• It was found that irradiation enhanced the corrosion rate of clad tube for both PWR and BWR.
Elmoselhi et al. (1994)	Hydrogen uptake mechanism	Heavy water	–	• Mobility of hydrogen species permeating through the oxide into the alloy depends on through-oxide-thickness distribution of intergranular porosity
Yamanaka et al. (1995)	Hydrogen solubility in zirconium alloys	Hydrogen gas	–	• For temperature below 850 °C, (α-phase) zircaloy-4 had the largest hydrogen solubility among zircaloy-2, zircaloy-4 and Zr–1%Nb
Garzarolli et al. (1996)	Clad corrosion behavior	Water and steam	–	• Nitrogen presence in BWR coolant increased the rate of nodular corrosion
Yamanaka et al. (1997)	Hydrogen solubility in zirconium alloys	Hydrogen gas	–	• In α-region, solubility of hydrogen was first found to increase with oxygen content and then the opposite trend was observed
Cox (2005)	In-reactor corrosion of zircaloy	Water and steam	–	• Alloying element redistribution fast neutron irradiation enhanced the corrosion in PWR
Kim et al. (2006)	Oxide and hydrogen on zircaloy clad behavior	Steam	–	• At high temperature ballooning is affected by oxygen as well as hydrogen Premature rupture is observed in high temperature ballooning
Lewis et al. (2009)	Fuel behavior at high temperature relevance to CANDU fuel	Heavy water	Helium	• Mechanisms responsible for clad failure were overstrain, low ductility, embrittlement due to oxygen, high strain rate, high fuel enthalpy, overstrain under oxide cracks

Cox (2005) did a broad review on different mechanisms of corrosion in water-cooled reactors during normal operation. He found that the mechanism of determining corrosion in zirconium alloys had changed a lot over the years. Following were his observations:

- The redistribution of alloying elements, especially iron, by fast neutron irradiation was found to be responsible for increased corrosion in PWRs.
- Galvanic corrosion due to residual potential differences between metallic phases existed in BWRs but not in high hydrogen concentrations PWRs.
- Crevice corrosion effect should be considered only when the geometry demanded it.

Maki and Ooyama (1976) observed that above 300 °C clad surface temperature, oxide film changed color from black to white, which resulted in lowering of film conductivity. The objective of their study was to verify the opinion that the hydride precipitated preferentially in regions of high tensile residual stress. It was found that hydrides were precipitated only when hydrogen absorption in the zircaloy exceeds beyond the terminal solubility limit at service temperature. Hydrogen presence beyond 500 ppm even at current

service temperature would embrittle the clad and therefore, as design practice, hydrogen absorption limit was 500 ppm and above.

Garzarolli et al. (1996) discussed the various aspects of clad failures, viz., the role of operating conditions, dimensional behavior of fuel rods and corrosion of zircaloy clads. The following were their observations:

- Gamma radiation affects the chemical nature of the environment, which may lead to defection of fuel rod.
- The concentration of free oxygen in the coolant differs strongly between BWR and PWR.
- The fuel rod deformation is a result of irradiation growth, anisotropy creepdown and pellet–clad mechanical interaction.
- In high temperature water or steam environment, a uniform oxide layer is formed on the clad surface.
- Also, a good surface finish and proper surface treatment strongly influence the corrosion behavior.
- A phenomenon called 'nodular corrosion' has been observed in BWRs and out-of-reactor experiments in high pressure steam above 400 °C. It is characterized by the formation of white pustules thicker than the uniform oxide film. These pustules grow together to form a very thick oxide layer. The presence of nitrogen in the coolant increases the rate of nodular corrosion.

Clad tube performance during reactor operation is largely dependent on its mechanical properties like yield stress, ultimate tensile stress, area reduction at fracture, creep rate. Pickman (1972) reviewed these properties of zircaloy-2 and observed a shift in their values due to texture change and deformation behavior, irradiation, hydrogen content in the tube and temperature. The following were observations:

- Highest ductility was obtained with annealed material in the temperature range 450–550 °C. Also, the maximum resistance to plastic instability was achieved using radial basal pole texture tube specimen.
- Hoop ductility was found to decrease under multi-axial stress loading.
- Irradiation strengthening for the annealed material would not fully saturate at fast neutron exposure lower than 10^{22} neutron/cm^2 and ductility was not reduced further after an exposure of about 5×10^2 neutron/cm^2.
- The presence of zirconium hydride up to 200 ppm at temperature about 200 °C. H_2 did not have any detrimental effect.

It was pointed out by Pickman (1994) that there was difference between the corrosion rate obtained in the laboratory test than that in actual in-reactor test. In fact, the corrosion level achieved in the laboratory was inferior in comparison to that inside the reactor due to the enhanced corrosion by irradiation. The observations were:

- In BWR applications, for clad surface temperature of 560 K the enhancement factor for corrosion due to irradiation is 10 whereas in PWR applications, for clad surface temperature of 630 K, it is 3 only.
- The parameters that may affect enhancement factor further are coolant composition and purity, flow velocity and coolant pressure, fast neutron flux, Zr/ZrO interface temperature and exposure time.
- The difference in enhancement factor for the two reactors PWR and BWR is also due to suppressing effect of H_2 in reducing the concentration of oxygen. Further the hydrogen absorption may cause the severe corrosion and affects the ductility of clad tubes due to formation of hydrides. The percentage of hydrogen absorption in PWRs is of 20–30% in comparison to 10% in BWRs.
- At BWR and PWR clad tube temperature, the terminal solubility limit of absorbing the hydrogen has been decided as 80 and 200 ppm respectively. It is found that damage to the oxide layer from spacer grids or other vibration source also caused its rapid localized corrosion termed as fretting corrosion.

During LOCA the clad tube surface is subjected to condition where coolant is partially absent. Hence, it is necessary to analyze the clad behavior in different environments. In several studies, experiments had been conducted with different surrounding conditions or environment. Emmerich et al. (1969) analyzed the clad behavior under loss of coolant accident with zircaloy-4 tubes in inert (argon gas) atmosphere as well as in steam environment. On the basis of their experimental data, following correlation was proposed for the evaluation of effective stress:

$$\sigma_e = 0.0113k' \exp\left[\frac{78,500 \pm 8900}{3.97RT}\right]\left(\frac{\dot{T}\varepsilon_l}{T^2}\right)^{1/3.97} \quad (1)$$

where $\dot{T}$ is the heating rate, K/s, ε_l is the logarithmic strain = $\ln(1+\varepsilon)$, and k' is 1 for tension tests and $(\sqrt{3}/2)^{1/3.97}$ for pressurized-tube tests.

The above correlation was valid for ductile expansion failure of zircaloy-4 in argon atmosphere.

Following were the findings:

- For inert atmosphere ductile expansion failure occurred in clad while in steam environment the fracture occurred with less expansion or ballooning in comparison to inert atmosphere.
- The failure may be either of brittle or ductile type depending on the internal pressure, temperature and amount of oxidation. In steam atmosphere, zircaloy-4 tubes with internal pressure above 8 bar, heated above 10 K/s, failed by ductile expansion whereas tubes pressurized at 6 bar failed by fracture at less than 34% expansion at hearting rates up to 200 K/s.

Furuta et al. (1978) conducted an experimental study on clad tube in steam and vacuum environments under LOCA like conditions. They studied the important aspects like diametral expansion, wall thinning and inner surface oxidation. The following had been observed:

- The maximum diametral expansion was very strong function of burst temperature. With increase in burst temperature from 700 to 830 °C i.e., in α-phase, there was an increase in the maximum diametral expansion. After that there was fall in the diametral expansion in the range 830–920 °C, i.e., in (α + β) phase. This behavior might be attributed to the phase transformation from α to β phase.
- From the literature review, they found that there was no effect of steam and inert atmosphere on maximum diametral expansion. Their own data revealed that maximum diametral expansion in vacuum environment was larger than that in steam environment for same burst temperature. It might be due to the presence of pre-oxidized layer on outer surface of clad.
- Ballooning in the clad was observed in the vicinity of 30 mm from center of rupture opening. Variation in wall thickness with ballooning was also observed which was dependent on heating condition.

Furuta and Motohashi (1980) further conducted X-ray diffraction (XRD) analysis on the oxide layers formed on outer and inner surfaces of the clad. The results from the above analysis showed that inner surface oxidation occurred due to rupture opening and this layer was found to be thicker and porous than that present on outside surface. Inner oxide film had higher content of hydrogen

due to the presence of tetragonal zirconia (ZrO) along with monoclinic (ZrO_2), while outside oxide layer had only monoclinic ZrO_2. One of the reasons of more hydrogen concentration in the inside layer was due to its inability to escape outside.

Inner surface oxidation of clad was also studied by Uetsuka et al. (1982) for the temperature range of 890–1194 °C in stagnant steam environment, which simulated the condition inside the ruptured cladding. The embrittlement of the specimen was primarily attributed to absorbed hydrogen by the zircaloy-4 clad tube. It was found that inside environment of clad tube affected its mechanical property especially the ductility. Zircaloy tube became brittle for more than 2.0 mg/cm^2 of weight gain (equivalent to 500 wt ppm) due to absorbed hydrogen. The study came with the same conclusion as reported by the earlier investigators that the inside environment conditions was strongly related to severe embrittlement.

Hindle and Mann (1982) studied the effect of steam environment on the clad behavior and compared it to that of without steam. The comparison of two different conditions was presented as convective cooling and radiative cooling, respectively. The maximum strain obtained in both the cases was of same magnitude except that the deformation pattern was different. In steam environment, a continuous increase in deformation was obtained in the flow direction of steam. The deformed shape appeared like of carrot for covective cooling whereas it appeared like sausage for radiative cooling. The convective cooling was considered as a mean to suppress the temperature variation in fuel elements which in turn controlled the deformation in axial direction. It was also found that:

- For clad tube assembly the internal pressure should be below 10 bars at any temperature in order to prevent the clad tubes to touch each other or from excessive bulging.
- Clad tube became more strengthened due to oxidation by steam and the strengthening effect was found to be more effective to the thinner region which had maximum strain.
- The heat transfer rate was found to be an important parameter to determine the deformation which in turn is dependent on the circumferential temperature variation.

The temperatures, at an axial location and around the circumference of the clad, differ significantly. This temperature difference is termed as azimuthal temperature difference and its effect on clad ballooning is an important parameter to study. Burman et al. (1984) performed a review on creep data, burst criteria, effect of oxygen on fuel clads during LOCA. They also performed a parametric study to study the effect of temperature, clad strain with time etc. from the model obtained from the review studies. It was observed that the eccentric arrangement of heater rod induced lesser strains in the clad tube as compared to the concentric arrangement. It might be due to the difference in azimuthal temperatures. It was recommended to include the effects of steam or air environments on cladding strain rates and strain localization to model the burst strain accurately in LOCA transients for cladding burst temperatures above 800 °C.

Lewis et al. (2009) have examined the CANDU fuel clad failure at high temperature on the basis of available literature. They have discussed the different aspects of clad deformation like oxidation, hydriding and embrittlement, the fuel–clad gap process and heat release, clad–fuel interaction and fuel behavior during power ramp. Following are the observations:

- The thermo-physical properties of zircaloy can be found from MATPRO database and has been used in the clad creep model NIRVANA code for ELOCA. It has been noticed that data on coefficient of thermal expansion above the β-phase transition temperature 1073 K are non-existent in the database.
- The places where clad and the fuel are in good contact due to pellet expansion or creep down of clad under coolant pressure, the value of high transfer coefficient is high and the temperature drop across the gap is less than 20 K.
- Average clad strain of 5% is taken clad overstrain failure criteria for ELOCA. It should be noted that this criterion represents onset of ballooning rather than clad failure.
- Under steam environment it has been noted that oxidation increases with the steam pressure for the temperature range of 700–900 °C. This pressure dependence does not seen at 1100 °C. For the oxidation of zircaloy-4 in the air and air + nitrogen atmosphere at temperature of 800 °C, there is a degradation of cladding material with the formation of zirconium nitride and its oxidation.
- Core re-flooding experiment reveals that hydrogen generation is dependent on degree of prior oxidation and re-flooding thermo-hydraulic conditions.

An experimental study on ballooning of clad, used in CANDU reactor, in the steam environment was undertaken by Sagat et al. (1984) covering the aspects like oxidation, cracking of the oxidized layers and localized deformation. It was observed that oxygen strengthened the zircaloy clad but reduced its ductility. The effect of oxidation on ductility was dominant above the 1300 K and cracks in oxide layer started to develop at strain of 1.6%. The number of cracks increased with the increase in hoop stress and heating rate.

Hofmann and Neitzel (1987) experimentally evaluated the cladding oxidation under severe fuel-damage condition, a combination of external and internal oxidation of the clad. The oxide layer found to obey the parabolic rate law initially. The oxygen diffusion into zircaloy clad surface was found to be the rate-determining measure. Due to oxygen diffusion, the embrittlement of clad took place and its rate was found four times faster for the case when either side of clad was subjected to oxidation in comparison to the case when only one side of clad was subjected to oxidation. In addition to oxygen, hydrogen absorption by clad tube is also one of reason of reduction in clad ductility. A number of studies have been dedicated to hydrogen absorption by the zircaloy clad tubes (Gulbransen and Andrew, 1957; Aronson, 1960; Shannon, 1963; Roy, 1964; Smith, 1965; Cox and Roy, 1965; Austin et al., 1974; Woolsey and Morris, 1981; Cox, 1985; Wart et al., 1991; Elmoselhi et al., 1994). A few have been discussed here:

Cox (1985) reviewed the mechanism of hydrogen absorption by zircaloy. He describes the mechanism of hydrogen gas absorption as molecular or dissociative adsorption of the hydrogen molecule at the oxide surface followed by permeation through the oxide. The diffusing species as well as permeation routes through the oxide were not very clear. Elmoselhi et al. (1994) described the mechanism as transport of hydrogen through the oxide and into clad tube during corrosion. Hydrogen solubility's in clad tubes for different alloys was studied by Yamanaka et al. (1995). Among three different alloys zircaloy-2, zircaloy-4 and Zr–1%Nb hydrogen solubility was found to depend on the temperature. It was found that for temperature below 850 °C, (α-phase) zircaloy-4 had the largest solubility not only among the above three but also higher than pure zirconium, whereas above this temperature all alloys had low solubility in comparison to pure zirconium. Further investigations on hydrogen solubility by Yamanaka et al. (1997) revealed that the pressure also had an effect on the solubility of hydrogen and with increase in pressure solubility was found to increase. It was also found that oxygen content also influenced the hydrogen solubility. In α-region, solubility of hydrogen was first found to increase with oxygen content and then the opposite trend was observed. How-

Table 5
Studies on creep.

Author (year)	Clad material	Outside/inside clad medium	Range of input parameters	Fuel simulator	Remarks
Gilbert et al. (1969)	Unalloyed zirconium	NA	Diameter = 6.35 mm, length = 50.8 mm	Section of rod is used	• Strain rate variation with temperature for different region were observed • Diffusion and dislocation glide were main creep controlling mechanism
Fiveland et al. (1977)	Zircaloy-4	Vacuum/argon	IOP = 25–100 bar, HR = 14, 28 and 42 °C	Heater rod	• Most of rupture occurred at the hot spot
Chung et al. (1977)	Zircaloy-4	Vacuum/argon	LOCA related conditions	Al_2O_3	• Most of circumferential expansion at rupture was observed due to localized ballooning
Erbacher et al. (1979)	Zircaloy-4	Steam/helium	IP = up to 100 bar, rod power = up to 50 W/cm	Al_2O_3	• Distribution of temperature was the prime factor regulating the zircaloy clad deformation mechanism
Rosinger et al. (1979)	Zircaloy-4	Inert	IOP = 9–1000 bar, T = 873–1973 K, HR = 50–100 K/s	NA	• Circumferential temperature variation had an impact on burst strain
Chapman et al. (1979)	Zircaloy-4 (unirradiated)	Superheated steam/helium	OD = 10.92 mm, t = 0.635 mm,	Heater rod	• Clad deformation was extremely sensitive to small temperature variation
Sills and Holt (1979)	Zircaloy-4	Steam	T = 700–1600 K, HR = 0–100 K/s	NA	• In all three phases of zircaloy diffusional, dislocation, and athermal creep were found Micro structural changes also affect the deformation
Bauer et al. (1979)	Zircaloy-4	Steam/helium	HR = 28 °C/s, ambient temperature = 343 °C	Hollow alumina pellets	• Tube burst ductility was found to be independent of the axial restraint
Erbacher et al. (1982)	Zircaloy-4	Steam/helium	IOP = 10–140 bar, HR = 1–30 K/s	Al_2O_3	• Burst strain reduction occurred in α-phase with increase in heating rate while in β-phase due to dominating effect of oxygen, increase in burst strain occurred with increase in heating rate
Matthews (1984)	Zircaloy	–	–	–	• The axial restraint prevent shortening of the tube and hence reduced the tendency to bend significantly
Ferner and Rosinger (1985)	Zircaloy-4	Steam/inert gas	HR = 1, 5, 10, 25 K/s, IP = 3–29 bar	Hollow alumina pellets	• Heating rate has minimal effect on burst strain in mixed phase
Arai et al. (1987)	Zircaloy-2	Atmosphere/argon	HR = 5, 20, 50, 100, 200 K/s, IP = 0.98–14.71 MPa	NA	• The LMP life fraction approach was used to predict clad failure at high-temperature conditions for BWR
Hong and Kim (1987)	Zircaloy-4	–	Experimental data from previous work	–	• Formula for strain rate sensitivity was obtained as $m_t = (1/(\sigma^* + \sigma_D))(\sigma^* m^* + \sigma_D m_D)$ • For percentage elongation or fracture strain measurement the derived expression was $\varepsilon_f = a m_t + b$
Picklesimer (1987)	Zircaloy	–	–		• Plastically strained clad tube give rise to elliptical cross section which is independent of amount of axial strain and process
Zhou et al. (2004)	Zircaloy-4 and Nb-modified Zircaloy-4	Argon	T = 723–773 K, stress = 40–100 MPa	Mandrel	• Both alloys had similar rupture characteristics
Kaddour et al. (2004)	Zircaloy-4 and Zr–1% NbO	Vacuum	Vacuum = 10^{-3}–10^{-4} Pa	NA	• In α region effect of dislocation and diffusion creep was found while in β region only dislocation creep was dominant
Kim et al. (2004)	Zircaloy-4	Steam/argon	IP = 100–600 bar, T = 600–1300 °C, HR = 1, 10, 100 °C/s	NA	• Clad deformation of was greatly influenced due to phase transformation
Seok et al. (2007)	ZIRLO	Atmosphere/argon	T = 365–570 °C	NA	• Burts creep properties were strongly related with the hoop creep properties
Lee et al. (2009)	Zircaloy-4 and Zr–Nb–Sn–Fe alloys	Atmosphere	T = 450, 480 and 500 °C, applied stress = 80–150 MPa	NA	• Tensile strength of Zr–Nb alloy was greater than that of Zr–Sn alloy.

ever, in β-region the dependency of hydrogen solubility was not completely understood and further investigations were suggested.

The effect on mechanical properties of zircaloy-4 clad due to absorbed hydrogen and oxide formation during LOCA was studied by Kim et al. (2006). The experiments for clad ballooning and thermal quenching were performed with 50 μm oxide thickness and 1000 ppm of hydrogen. The following was the outcome of the study:

- Ballooning of pre-oxide clad tube at high temperature was affected by seizing the intra-granular deformation of α-phase below 700 °C and accommodating the local oxide growth above 900 °C.
- Ballooning of pre-hydride clad tube at high temperature was affected by the ductility recovery in the β-phase and induction of hydrogen embrittlement leading to failure.
- Threshold ECR of the pre-oxidized cladding was in the range of 20%, similar to the pre-hydride cladding.
- The ductility of the quenched cladding was found to decrease when the absorbed hydrogen reached 1000 ppm due to the increased presence of oxygen in the residual β-phase layer.

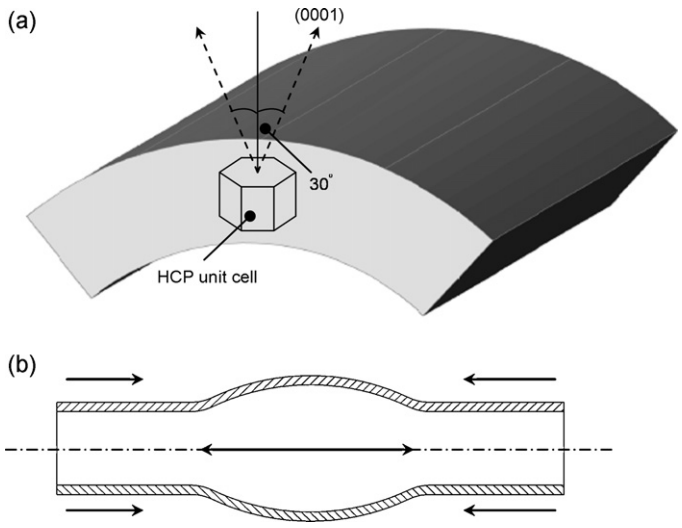

Fig. 7. Anisotropy (a) clad tube element (b) axial contraction (Hindle and Mann, 1982).

Table 6
Different creep controlling mechanism.

Region	Temperature (°C)	Creep rate controlling mechanism
A	50–300	Interaction of dislocation with oxygen impurities
B	300–400	Dislocation intersection
C	400–500	Dislocation intersection with precipitates
D	500–700	Combined impurity atoms
E	700–800	Grain boundary diffusional creep
F	800–850	Non-conservative jog motion in screw dislocations

After presenting the review of corrosion studies, the next section is being dedicated to the failure mechanism that occurs during LOCA and it is the plastic deformation or creep.

3.1.2. Creep

The time-dependent permanent deformation is termed as 'creep' due to constant load or stress. The phenomenon of creep is more pronounced in materials that are subjected to heat for long periods. Creep is a function of temperature. It increases with the temperature. During reactor operation and LOCA situations, clad tubes are subjected to elevated temperature and at the same time exposed to stresses. During the normal plant operation, the fuel clads remain in α-phase and transition phase whereas β-phase is reached only during an accident scenario. In α-phase, HCP structure causes the deformation of clad tube in both circumferential as well as axial direction with different strain values, as shown in Fig. 7. This leads to anisotropy in α-phase during normal reactor operating condition. However, in β-phase because of BCC structure during loss of coolant accident, the clad material behaves isotropically. This means that during LOCA, in α-phase, the creep anisotropy will result in shortening of the tube whereas in β-phase the tube will not suffer any significant change in length due to isotropic effect (Furuta et al., 1978).

Table 7
Creep rate equation for three phases.

Phase	Temperature range (K)	Creep rate equation, s^{-1}, $\{\dot{\varepsilon}_{ss} = A\,\sigma^n \exp(-Q/kT)\}$
α	940–1073	$2000\,\sigma^{5.32}\exp(-284{,}600/kT)$
(α + β)	1140–1190	$6.8\times10^{-3}\,\sigma^{1.8}$ $\exp(-56{,}600/kT)$ for creep rate $\leq 3\times10^{-3}\,s^{-1}$
β	1273–1873	$8.1\,\sigma^{3.79}\exp(-142{,}300/kT)$

Table 5 provides the summary of creep studies in the chronological order. Gilbert et al. (1969) conducted uni-axial tension test to understand the creep behavior of unalloyed zirconium in the temperature range of 50–850 °C (α-phase). For the better understanding of creep behavior of clad tubes, they suggested six different creep domains having distinct temperature bands. Each domain of creep is governed by a unique creep controlling mechanism, as shown in Table 6. Following were their observations:

- Impurities like O_2 and β-annealed structure provided greater creep resistance and strength than α-annealed structure.
- It was suggested that the mechanisms that govern the plastic deformation would be same for zirconium as well as in zirconium alloys.

The steady-state creep behavior of zircaloy-4 clad was studied by Rosinger et al. (1979) in the temperature range of 940–1873 K. They performed a uni-axial creep test in an inert atmosphere to obtain the creep data for zircaloy-4 clad. The steady-state creep equation was developed using the following equation:

$$\dot{\varepsilon}_{ss} = C\exp\left(-\frac{Q}{kT}\right) \quad (2)$$

where Q is the activation energy, k is the gas constant, T is the cladding temperature in Kelvin.

The steady-state creep rate equations for all the three phases-α, α + β and β were obtained by applying Arrhenius power law on the test data obtained, as shown in Table 7.

The following were the results:

- The strain rate was found to increase with surface temperature.
- In mixed-phase region, due to lack of data, the creep rates greater than $3\times10^{-3}\,s^{-1}$ could not be predicted.
- At higher temperature, no major difference in zircaloy-4 (SRA or stress relieved annealed) and zircaloy-2 (RXA or recrystallization annealed) creep data was found while at lower temperature, the difference was due to fabrication.

In many alloys, the strain rate sensitivity becomes negligibly small in the temperature range of dynamic strain aging. It was suggested by Hong et al. (1983) that oxygen atoms were responsible for low strain rate sensitivity and less elongation. Hong and Kim (1987) derived an equation which could predict the temperature dependence of the elongation for clad tube of zircaloy-4. The prediction from proposed equation was found in good agreement with their own experimental data. The low strain rate sensitivity due to dynamic strain aging produced by oxygen was found to decrease the ductility in flow stress plateau region. Above the flow stress plateau temperature range, the elongation of alloy occurred rapidly.

The normal operating zircaloy maximum clad surface temperature remains about 400 °C (for BWR ~ 300 °C, for PWR ~ 350 °C and for CANDU <300 °C) whereas the temperature reaches above 1000 °C during LOCA. As such, the clad undergoes phase transformation. Stress and strain behavior of the clad is different in different phases. Fiveland et al. (1977) carried out an experimental investigation on clad tube to simulate the coolant-loss condition with complete loss of coolant. The test data, thus, obtained was useful for analytical study. They observed that rupture position was normally distributed about the point of maximum temperature. However, angular and axial distribution of rupture was dependent on mode of testing. Following observations about the transition phase (α + β) were made:

- Transition phase found to have strong effect on ductility at rupture.

- Clad rupture temperature was found to vary linearly with hoop stress.
- The ductility reached to a minimum at the center of transition phase followed by an increasing trend.

Chapman et al. (1979) tested zircaloy-4 clad in superheated steam condition, a stage occurred during LOCA. Clad deformation was extremely sensitive to the small temperature variation. And the observations were:

- Lesser clad deformation was found in this environment in comparison to inert atmosphere.
- In α-phase, deformation was found out to be a function of temperature variation around the circumference and for uniform temperature variation larger deformation was obtained.
- Further, in α-phase the total circumferential elongation (TCE) was dependent on texture, local temperature variation, and heating rate while in β-phase or higher temperature range oxidation had the dominating effect.

From the above observation it was concluded that oxidation was responsible for failure at high temperature while wall thinning was found as reason of failure at low temperature.

Sills and Holt (1979) had developed a model for transient plastic deformation of clad especially for zircaloy-4 during LOCA based on multi-component theory. Three creep mechanisms, viz. diffusional creep, dislocation creep, and athermal strain, were responsible for clad deformation during LOCA. Total plastic strain was calculated as the summation of strains due to all three deformation mechanism. The data used were based on the temperature range of 700–1600 K with heating rate varying from 0 to 100 K/s and strain rate from 10^{-5} to 10^{-1} s^{-1}.

As a consequence of LOCA, the deformation of clad causes the coolant flow blockage and establishes contact between the adjacent clad tubes in fuel bundle. Hence, total tangential strain and time of failure are the important parameters to be investigated. Circumferential temperature difference is one of the factor that influences the above two parameters. Ferner and Rosinger (1985) carried out clad tube failure study in steam environment with circumferential temperature difference as one of the parameters. The study was done for α + β and β phases of clad tube only. In α-phase and lower (α + β) phase regions, lower tangential strain was obtained for larger value of circumferential temperature difference while higher tangential strain was obtained for smaller circumferential temperature difference for clad tube temperature up to 1200 K.

Kim et al. (2004) performed isothermal ballooning and transient ballooning test on zircaloy-4 clad tube in steam environment. In isothermal ballooning test, the percentage elongation was found to increase with temperature in α-phase and peak was achieved in the same phase itself. With the onset of the transition phase (α + β), there was a sudden fall in the percentage elongation with an increase in temperature and then it stabilized to a constant value in the β-phase. The reason was that in α-phase region, creep deformation was due to both glide dislocation and climb dislocation. The peak in total elongation was due to grain deformation caused by dislocation glide and the grains were circumferentially elongated due to anisotropy. In β-phase, the circumferential elongation was restricted and an increase in temperature led to the development of thick oxide layer; incapable of bearing high load or stresses. Subsequent cracking in oxide layer caused the failure of clad tube. In transient heating test, on the other hand, there was a decrease in percentage elongation with temperature in α phase. The minimum value of percentage elongation was obtained in the transition phase (α + β) at 900 °C. With temperatures above 1000 °C, there was a sharp rise in the percentage total elongation until 1150 °C. After that, the percentage total elongation again started to reduce. In α-phase, the rupture opening was circumferential as well as axial while in β-phase, the rupture opening was restricted to only in axial direction.

The clad tube ends are welded with the end plates in a fuel bundle. The end plates provide axial constraint in clad tube and affect the clad tube expansion in circumferential direction. The clad failure due to the effect of end-constraints has been shown in Fig. 7. One such study was done by Chung et al. (1977). They observed that for unconstrained clad tube larger circumferential strain occurred in comparison to constrained clad tubes. For the rupture temperature range of 700–850 °C (α-phase), the effect of axial constraint was greater on rupture circumferential expansion. The contraction in the clad tube was due to anisotropy of hexagonal closed packed structure (HCP). Due to this contraction decrease in circumferential strain of clad tube is found. It has been found that effect of heating rate on burst temperature for maximum circumferential strain depends on clad surface temperature. Up to 820 °C burst temperature decreases with decrease in heating rate while above the 900 °C no effect of heating rate on burst temperature is found.

Bauer et al. (1979) concluded that the transient heating tube burst tests of spent fuel cladding did not provide any significant evidence of differences in behavior between irradiated and unirradiated zircaloy claddings. Tube burst ductilities were found to be independent of the axial restraint.

Matthews (1984) developed a mathematical model to study the effect of anisotropy of zircaloy clad ballooning. His model was based on the assumption that the cross-section of clads remained circular during the ballooning process. The assumption was bold in a sense that experiments had already confirmed that deformed specimens had elliptical cross-section. It was found that anisotropy had small effect on time of failure and degree of localization failure strain. However, environmental conditions had greater effect. Further, it was found that the axial restraint prevented shortening of the tube, thus reduced the tendency to bend significantly.

Picklesimer (1987) presented a comprehensive description on anisotropy in zircaloy. Apart from classifying anisotropy, he also discussed the analytical model originally proposed by Hill (1948). The theory was based on the following conditions:

- The axes of anisotropy
  - must be definable in the material,
  - are so located that the uni-axial tests can be conducted along them
- The mechanical properties must remain the same in tension and compression along an axis but may vary with axial orientation.

Erbacher et al. (1979) performed experiments on zircaloy-4 tubes up to 100 bar pressure using air as well as steam as surrounding environment emphasizing on ballooning behavior for single as well as bundle geometry. It was observed that:

- From a single rod test, for non-uniform circumferential temperature variation, the clad would swell asymmetrically accompanied with bending. The circumferential elongation occurred due to wall thinning of tube restricted only to a small part of entire circumference. Early burst occurred at a point having highest temperature after circumferential elongation despite of much larger local strain.
- Anisotropic behavior of clad tube caused axial contraction of tube along with circumferential elongation which, in turn, decreased the gap on hotter side and increased on cooler side.
- Smaller the circumferential temperature difference larger would be the strain and vice versa is also true.

Erbacher et al. (1982) further simulated the clad tube burst experimentally and it was that for all three phases (α, α + β, and

β) increasing the internal over-pressure resulted in decrease in burst temperature for same heating rate, whereas with increase in heating rate burst temperature increases. Further it was established that heating rate had greater impact on burst stress–strain in (α + β)-phase and β-phase in comparison to the α-phase. In α-phase increasing heating rate resulted in the reduction of the burst strain while in β-phase due to dominating effect of oxygen, increase in burst strain was observed with increase in heating rate. They developed and validated the burst criterion model for steam environment, which could be applicable to both uniform as well as non-uniform temperature distribution with overpressure in the range 10–140 bar and heating rate in the range 1–30 K/s. The burst stress was modeled as a function of the burst temperature and oxygen uptake in the following equation:

$$\sigma_{\theta B} = a\exp(-bT)\exp\left[-\left(\frac{(100O_x - 0.12)}{0.095}\right)^2\right] \quad (3)$$

where a and b were determined experimentally.

Failure model for zircaloy-4 clad tube was also developed by Rosinger (1984) for inert as well as steam atmospheres for temperature range of 900–1600 K with an assumption that failure occurred when tangential stress reaches the burst stress. For steam atmosphere, he used Erabacher et al. [31] correlation, represented by Eq. (1). However, for inert atmosphere the following correlation was proposed with burst stress, $\sigma_{\theta B}$, as a function of burst temperature, T_B:

$$\sigma_{\theta B} = a\exp(-bT_{\theta B}) \quad (4)$$

where constants 'a' and 'b' have different values for different phases, viz. α, α + β, and β phases. It was found that clad tube failure was affected by parameters like anisotropy, heating rate, oxidation and circumferential temperature variation. Following were his conclusions:

- With decreasing stress, there was an increase in burst temperature.
- In α-phase, with the increase in either the anisotropy or the heating rate, the increase in burst temperature and decrease in burst strain were resulted.
- The effect of oxidation was significant in β-phase region. As such, the highest heating rate yielded highest burst strain.
- The clad failure would occur at a place on its circumference, where temperature was maximum.
- The burst strain reduced with the rise in circumferential temperature difference.

Arai et al. (1987) conducted thermal transient, isothermal, and thermal transient-isothermal experimental tests on zircaloy-2 clad tube for LOCA like situation. They developed correlations for the above three tests using Larson–Miller parameter (LMP) approach:

For isothermal test

$$\mathrm{LMP} = T(\log\, t_f + C) \quad (5)$$

where T is the absolute temperature, t_f is time to failure and C is constant having value 20.

For thermal transient test

$$\left(\frac{10^{20}}{\dot{T}}\right)\int_{T_i}^{T_B}\exp\left(-\frac{2.303\,LMP}{T}\right)dT = 1 \quad (6)$$

where T_i is the initial temperature, $\dot{T}$ is the heating rate and $T = T_i + \dot{T}_t$.

For thermal transient-isothermal test

$$\mathrm{LMP}\times 10^{-3} = -8.8247\times 10^{-6}\ \ \sigma_{\theta t}^3 + 1.8987\times 10^{-3}$$
$$\sigma_{\theta t}^2 - 0.17296\sigma_{\theta t} + 23.445 \quad (7)$$

where $\sigma_{\theta t}$ is tensile hoop stress in MPa and is valid for 6.5–100 MPa.

It was observed that the burst temperature was found to increase with decreasing internal pressure whereas at same internal pressure, burst temperature was found to increase linearly with logarithm of heating rate. For isothermal test, time of burst was found to decrease with increase in internal pressure and temperature. In thermal transient-isothermal test, the time of burst was found to decrease with higher holding temperature.

Kaddour et al. (2004) compared the clad deformation mechanism for zircaloy-4 and Zr–1%NbO alloy. It is observed that phase-transformation from α to β started at 820 °C for zircaloy-4 whereas at 770 °C for Zr–1%NbO alloy. They proposed that the creep behavior in both α and β phases was best described by power-law given by the following equation:

$$\dot{\varepsilon}_{ss} = \frac{A}{T}\sigma_\theta^n\exp\left(-\frac{Q}{kT}\right) \quad (8)$$

and in mixed phase region (α + β) by the following simplest equation:

$$\dot{\varepsilon}_{ss} = B\sigma_\theta^n \quad (9)$$

In β-phase domain Zr–1%NbO was found to have more creep resistance in comparison to zircaloy-4 and low creep resistance in α-phase and (α + β)-phase domain. Different phases exhibited different creep mechanisms. In α region dislocation and diffusion creep was observed while in β region only dislocation creep was dominant. For mixed-phase region further investigation was suggested. Zhou et al. (2004) compared the properties of zircaloy-4 and niobium induced zircaloy-4. He found that both alloys had nearly similar rupture characteristics. The deformation behavior ZIRLO, was experimentally analyzed by Seok et al. (2007). They suggested obtaining more creep data for different temperature ranges, especially for high temperature regions as the creep mechanisms had been found to vary with temperature. Recently, a comparison of properties for Zr–1% Nb and zircaloy-4 has been done by Lee et al. (2009). The tensile strength of Zr–Nb alloy is found to be greater than that of Zr–Sn alloy due to more strengthening effect by Nb at high temperature. While creep resistance of Zr–Sn is more than the Zr–Nb due to dominating effect of solution strengthening of Sn.

3.2. Reactivity-initiated accidents (RIA)

The reactivity-initiated accident (RIA), although exceedingly rare, occurs when there is an unwanted increase in fission rate and reactor power due to unexpected removal of control rods or media. This rise in power leads to the damage of reactor core and, sometimes, causes the disruption of the reactor, as happened in Chernobyl. The rise in power excursion leads to the failure of clad tube and release of radioactive material into the reactor coolant. In severe cases, fuel dispersed into the coolant after the shattering of clad tubes. The inclusion of hot fuel in coolant leads to the formation of steam and rise of pressure, which ultimately results in the damage of other components, fuel assemblies and possibly also the reactor pressure vessel. Clad tube behavior under RIA depends on the characteristics of the power pulse, core coolant condition, burn-up-dependent state of the clad tube, and clad tube design. The research work on RIA started only after the accident in Chernobyl nuclear reactor. The post-accident investigations established that the accident was due to the uncontrolled reaction. The fuel pellet behavior during RIA can be divided into the following three phases:

Phase-I: It includes the sudden rise in temperature of fuel element and its thermal expansion along with release of fission gases, which in turn, increases the clad tube temperature at a very high rate. During this phase, the clad temperature remains below the value of 600 °C. The clad is subjected to multi axial loading due

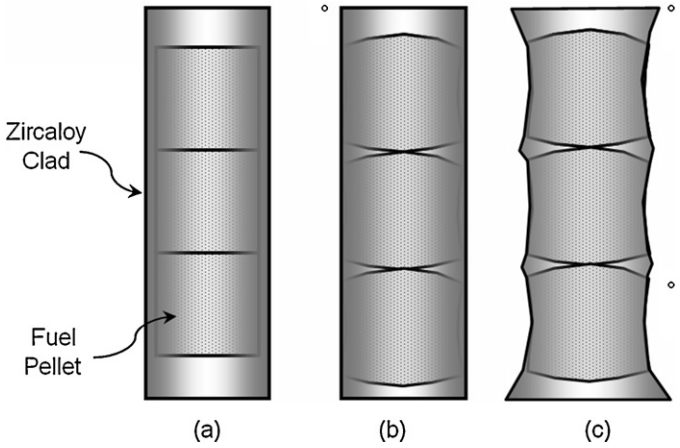

Fig. 8. Schematic diagram of pellet–clad mechanical interaction.

to fuel displacement. The clad failure due to pellet–clad mechanical interaction (PCMI) in this phase depends on the clad condition properties like irradiation damage, oxide layer thickness, hydride concentration.

Phase-II: In this phase, further rise in clad temperature takes place. The clad temperature remains in the range 1000–1200 K for 10–15 s. During the temperature rise, there is deterioration in the clad stiffness, which ultimately results in deformation and rupture (Cacuci, 2010).

Phase-III: In this phase, usually the re-flooding is activated and as a result, the high temperature clad tube surface is quenched, which leads to fragile fracture of clad. The fuel rod gets exposed to the surrounding due to the crack formation.

The failure of clad tube due to RIA, in general, can be divided into two categories; (1) clad failure due to PCMI, which occur at the early heat-up phase of the accident at low temperature, with high burn-up, and (2) clad failure associated with departure from nucleate boiling, which occur at later stage of the accident and also termed as high temperature failures. The second type of failure has not been studied much. The failure due to PCMI has been discussed in details in the next section. However, DNB has been discussed separately.

3.2.1. Pellet–clad mechanical interaction (PCMI)

Fig. 8 shows the stage-wise PCMI an interaction leading to the clad deformation. Fig. 8(a) represents clad and fuel under normal operating condition. The coefficient of thermal expansion of UO_2 fuel is more than that of zircaloy clad. Further, fuel being at higher temperature (~1600 °C) than the zircaloy clad (~300 °C), the fuel pellet will touch the clad tube, as shown in Fig. 8(b). During the process, the fuel pellet undergoes change in shape, characterized by the formation of ridges at the pellet–pellet interface. As the fuel touches the clad, its temperature rises and it takes the shape of the deformed pellets, as shown in Fig. 8(c). The cracks will appear on clad tube surface and finally clad failure takes place. The mechanical interaction of the fuel pellet and the zircaloy clad depends upon gap size, burn-up, friction coefficient between clad and pellet (Steinar, 1972).

Some of the important studies involving pellet–clad mechanical interaction has been presented in Table 8. Steinar (1972) gave an insight into the mechanism of cladding deformation occurred due to its interaction with fuel pellets. He did an experimental investigation on clad for BWR applications and found that:

- Maximum strain in axial direction could be over 2%; 1% could be quite normal at a heating rate of 600 W/cm. The circumferential strain of 1% could be expected.
- The interaction of fuel pellet with the clad was found to take place between 200 W/cm and 500 W/cm. This heat rating was expected to shift to lower value with time.
- Strains were proportional to heat load.
- When the in-reactor creep rates are appreciable fuel–clad interaction starts instantly resulting in large strains in the cladding.
- Additional strains were introduced due to the formation of cracks in the fuel pellet.

Lustman (1979) pointed out that iodine produced as a fission product corroded the clad from inside and was responsible for the crack penetration through the full clad thickness. The appropriate combination of parameters like stress, exposure time, and iodine concentration was found to be responsible for the failure. As remedy it was suggested that the temperature of the fuel could be minimized by reducing the fuel rod diameter, which would limit the production of iodine. Sidky (1998), Jacques et al. (1999) and Lewis et al. (2011) are other important review studies on iodine-induced stressed corrosion cracking.

It has been established that zircaloy claddings during fuel–clad interaction stress are susceptible to stress-corrosion cracking in an environment containing the iodine. Pickman (1994) in his paper talked about the causes of iodine stress-corrosion cracking and suggested the possible remedies. According to him, the causes were mainly from the movement of control rods, peaking factors due to partial reloads and following power demands. The remedies proposed were:

- Reduction of fuel rod diameter,
- use of bore surface lubricant on inside of clad to reduce relative friction,
- use of hollow, shorter and duplex fuel pellet,
- use of multiple crack initiators on the fuel–pellet surface,
- by reducing the iodine availability, achieved by reducing fuel rod diameter, use of increased helium pre-pressurization and rifled bore cladding.

Coleman (2002) had experimentally simulated the pellet–clad interaction to imitate the complicated reactor situations. He conducted the swelling test to devise a method for increasing the tolerance of the clad due to power ramps. The core of fuel rod was simulated by means of aluminum rod surrounded by ceramic liner (Al_2O_3) which touched the clad on other side. To produce swelling compressive force was applied about its axis and its expansion in radial direction deformed ceramic annulus. This technique was later adopted for CANDU fuel in which a graphite layer was placed inside surface of clad which helped to increase the ductility of fuel cladding and prevent the bursting during power ramp.

Hannerz and Vesterlund (1975) touched the durability aspect of zircaloy clad material with a special focus on fuel–clad interaction type of failure. Following were their observations:

- Annealing improved the ductility of zircaloy clad and made it resistant against fast power changes.
- Use of recrystallized annealed material with the texture angle of about 30° between the basal poles and surface normal was recommended for BWR while for PWR annealed material with changed texture angle to 45° was recommended.
- It has been found that annealed clad has higher creep strength at lower creep rates.

When clad tube has served for high burn-up at high heat transfer rate, mechanical interaction between cladding and fuel is considered as the most probable reason of clad failure. Hence, extents of clad tube deterioration including its deformation during service conditions are also necessary. Lee et al. (2001) studied the ductility

Table 8
Studies on pellet–clad interaction.

Authors (year)	Aspect	Remarks
Steinar (1972)	Pellet–clad mechanical interaction	Maximum stress occurred in circumferential direction due to PCI and strain produced due to PCI was suggested to be proportional to heat load
Hannerz and Vesterlund (1975)	Manufacturing effect on zircaloy properties	PWR annealed material with texture angle of 45° was recommended for PWR to resist creep while 30° texture angle for BWR
Lustman (1979)	Pellet–clad mechanical interaction	Stress corrosion crack in the clad occurred due to PCI and presence of iodine in environment further worsen the situation by acting as corroding agent
Pickman (1994)	PCMI and clad corrosion behavior	Iodine was released during reactor operation due to control rods movements, peaking factors due to partial load and power demands
Lee et al. (2001)	Effect on clad properties due to PCMI	Elongation or strain rate sensitivity of clad was not only the function of temperature alone but oxygen had also an influence on it
Coleman (2002)	Simulating the clad failure due to fuel expansion	To prevent the clad failure from fuel interaction the relative friction between fuels and clad was recommended to decrease.
Saux et al. (2009)	Clad behavior and failure due to various stress states	Hydrogen has no impact on plastic anisotropy but the temperature has an effect on it

and strain rate sensitivity of zircaloy-4 for the case of interaction between pellets and clad. It was found that elongation or strain rate sensitivity of clad was not only the function of temperature alone but oxygen had also an influence on it. Oxygen caused the decrease in strain rate sensitivity and minimum strain rate sensitivity or elongation minimum was achieved with which ductility of clad was found to decrease. However, with increase in temperature range above the flow-stress plateau rapid elongation in the alloy was observed. For CANDU fuel, ductility loss due to dynamic strain-aging had been observed in the temperature range of 250–400 °C.

Effect of pellet–clad interaction on anisotropic plastic behavior of cold-worked stress zircaloy-4 clad failure during RIA has recently been undertaken by Saux et al. (2009). It has been found that plastic anisotropy is not affected by hydrogen but the temperature has an effect on it. Decrease in material strength with temperature increase has been observed while reverse pattern has been observed for ductility having higher value in circumferential direction in comparison to axial direction. Effect of hydrogen content on ductility above 350 °C has not been observed.

3.2.2. Departure from nucleate boiling (DNB)

As the coolant flows past the fuel bundle, it picks up heat from clad tubes surface. During RIA, the increased reactivity causes the heat flux to rise unexpectedly to reach its critical value. The coolant which initially underwent nucleate boiling under normal operation, suddenly starts departing from it. The large bubbles form and a condition is reached when the steam bubbles no longer break away heated tube surface. The vapor bubbles form an insulating layer on the clad surface and there is a decrease in heat flux. This drop in heat flux is termed as departure from nucleate boiling (DNB). It is also known as unstable film boiling or partial film boiling. During DNB, the surface temperature must therefore increase substantially above the bulk fluid temperature in order to maintain a high heat flux. Avoiding the critical heat flux (CHF) is an important engineering problem in heat transfer applications especially in nuclear reactors, where fuel clads must not be allowed to overheat. DNB can be avoided by either way, increasing the coolant pressure or increasing its mass flow rate or both.

3.3. Criteria for ECCS for CANDU type reactors

During LOCA, the circumferential elongation of clad along with axial constraint causes the clad bursting in the absence of sufficient cooling. The emergency core cooling system (ECCS) is actuated as soon as the LOCA is detected in the reactor. The sudden supply of water, termed as re-flooding, is activated to cool the reactor core. The volumes of work have been published on the acceptance for ECCS and some are mentioned in Table 9.

After re-flooding in the calandria tubes with the activation of ECCS, quenching of clad tubes causes the brittle fracture at the circumferential oxide layer crack. In most of the cases, the fracture occurs only at one position. The various criteria have been reported in the literature for zircaloy clad embrittlement due to rewetting. The Sawatzky criterion was specifically used as the rewet failure criterion in the ELOCA transient code. According to this criterion, if the oxygen concentration over half of the clad wall thickness exceeds ~0.7 wt%, the clad tube can fail upon rewet during the introduction of emergency core cooling system (Sawatzky, 1979).

Clad tube integrity and fracture shape of zircaloy-4 clad after re-flooding was studied by Uetsuka et al. (1983). From the experiments performed for both unrestrained and restrained conditions, the equivalent cladding reacted (ECR) was found to be different in each case. For unrestrained condition, ECR for clad tube fracture reached to 35–38% while for restrained case, the value was in between 19 and 24%. From above limits for both unrestrained and restrained it was concluded that 15% ECR of acceptance criteria (Japanese limit) for ECCS. Hydrogen absorbed might be one of the reasons of fracture under re-flooding since the amount of hydrogen at the fracture positions was found to be too high in comparison to that in the region near to rupture. Furuta et al. (1984) had also performed an experimental study to verify the embrittlement criteria of zircaloy clad tube for LOCA situation. It was found that maximum clad temperature of 1200 °C and 15% ECR value for zircaloy clad during LOCA was sufficient to activate ECCS. Further it was found that rupture opening for single rod burst test was smaller in comparison to the opening in multi-rod burst test. Hence, the hydrogen absorption is also one of the important criterions for clad tube during LOCA situations.

Pickman (1994) mentioned in his review paper some important aspects of postulated LOCA conditions. These aspects were (1) the time–temperature transient experienced by the clad during the re-flooding (2) differential pressure across the clad during the process. According to the study, the transient phase had a blowdown phase of 20 s followed by refill and re-flood phases of about 300 s. The rise of clad temperature took place and reached a peak value in the blowdown phase after 50–100 s. It was found that during LOCA, clad diameter increased by 100% and most of the maximum clad strains occurred at a temperature of about 1125 K.

Erbacher and Leistikow (1987) reviewed the experimental works pertaining to the establishment of acceptance criteria for 'emergency core cooling system (ECCS)' in LOCA of light water reactors (LWRs). They also reported the effect of air environment on the ductility of zircaloy-4 clad. It was concluded that air was an inadequate medium to study oxidation at temperatures above 900 °C with respect to mechanical behavior, since air grown scales did not exhibit load bearing capability. For oxygen uptake in clad tube and combined layer growth (ZrO_2, α-Zr (O)) followed the

Table 9
Studies on criteria for emergency core cooling system.

Author (year)	Aspect	Remarks
Sawatzky (1979)	Zircaloy-4 embrittlement criterion for CANDU fuel	The rewet failure criterion in the ELOCA transient code (where if the oxygen concentration over half of the clad wall thickness exceeds ~0.7 wt%, it can fail upon rewet during the introduction of emergency core cooling)
Uetsuka et al. (1982)	Zircaloy-4 embrittlement due to oxidation in steam	For unrestrained condition, ECR for clad tube fracture reached to 35–38% while for restrained case, the value was in between 19 and 24%
Furuta et al. (1984)	Zircaloy clad burst behavior under LOCA	Maximum clad temperature of 1200 °C and 15% ECR value for zircaloy clad during LOCA was sufficient to activate ECCS
Erbacher and Leistikow (1987)	LOCA effect on Clad behavior	ECCS cooling effect increased the temperature difference on clad tube circumference
Pickman (1994)	Zircaloy performance in LWRs	During LOCA, clad diameter increased by 100% and most of the maximum clad strains occurred at a temperature of about 1125 K
Chung (2005)	Fuel behavior Under LOCA	Peak Cladding temperature should not exceed 1204 °C
Nagase et al. (2009)	High burn-up fuel clad behavior under LOCA	At fracture ECR value has been found to be in the range of 27–38% much higher than the 15% ECR value for low burn-up fuel clad

parabolic path with respect to time above 1000 °C. The 17% oxidation amount obtained by Baker–Just correlation is in consistent with the experimental data to set ECC criteria and remain valid after enhanced pre-oxidation and transient exposure at maximum temperature measured at 10 min, 1200 °C. During Cladding-steam oxidation reaction parabolic kinetic correlation is used for oxygen gain (increase of ZrO_2 thickness growth) in clad. Arrhenius correlation is used to define the reaction rate as a function of temperature

$$\dot{O}_x = A_m \exp\left(-\frac{Q}{kT}\right) \tag{10}$$

$\dot{O}_x$ is the oxygen mass gain rate in mg/cm^2/s$^{1/2}$, A_m is the pre-exponential factor, Q is the activation energy, k is the universal gas constant, and T is the cladding temperature in Kelvin.

It should be noted that the laboratory corrosion experiments that underlie parabolic kinetics in the above equation for zircaloy oxidation are isothermal, usually conducted in unlimited steam environments, and are restricted to metal specimens whose thickness is large compared with the scale thickness. However, a moving boundary diffusion model is a more general approach, which particularly becomes important under reducing conditions where the oxide scale can disappear (which the parabolic model cannot predict).

For Kinetics of high temperature oxidation for zircaloy Baker–Just equation is given by

$$w = 2029t^{0.5} \exp\left(\frac{-11,450}{T}\right) \tag{11}$$

where w is the zirconium metal weight reacted per unit surface area in mg/cm^2, T is the temperature in K, t is the time in seconds at constant T.

The data obtained from out-reactor test was found in line with in-reactor data. It was established that nuclear environment had no influence on clad deformation. Mechanical properties like embrittlement and creep were affected by oxidation, the amount of oxygen and hydrogen uptake and its distribution in the clad tube. The cooling effect of the ECCS resulted in an increase in azimuthal temperature differences on clad surfaces. This ultimately resulted in limiting the average circumferential burst strain in bundles up to 50%. It was also reported that the results of bundle test were in line with those of single tube and did not indicate any influence of nuclear environment on cladding deformation.

Chung (2005) has reviewed the present LOCA related acceptance criteria for ECCS of LWRs. It has the following requirements:

(a) peak cladding temperature must not exceed 1204 °C,
(b) maximum cladding or equivalent cladding reacted (ECR) must not exceed 17% of clad thickness.

An improved correlation was given by Cathcart et al. (1977)

$$w = 601.8t^{0.5} \exp\left(\frac{-10,050}{T}\right) \tag{12}$$

Both correlations agree well in 800–1000 °C range while in 1100–1200 °C there is a difference of 50 °C in favour of Cathcart–Powell correlation. 17% ECR value is obtained as acceptance criteria for ECCS.

(c) maximum hydrogen generation is limited to 1%,
(d) core geometry must be coolable,
(e) ECCS must be designed for long term cooling.

Nagase et al. (2009) have recently analyzed the clad behavior with samples of newer clad materials having burn-up ranging from 66 to 76 MWd/kg. This amount of burn-up has no significant effect on clad oxidation, rupture, and ballooning behavior. The ECR value at fracture has been found to be in the range of 27–38% much higher than the 15% ECR value for low burn-up fuel clad which should be consider before deciding the acceptance criteria for high burn-up fuel clad.

3.4. Core-degradation phenomena

The core degradation phenomenon is a consequence of either LOCA or RIA and comes under the category of 'beyond design basis accidents (BDBA)'. This may happen due to multiple failures of safety systems. Such category of accidents leads to degradation of the core, in which the integrity of many or all of the barriers to the release of radioactive material is in jeopardy. The core degradation is the step-wise processes of melting and liquefaction of core of the reactor. The core degradation ultimately leads to severe accident. The in-vessel degraded core phenomena is important for the purpose formulating measures for accident management, assessment of the risk involved and recommendation for the safer design of next generation of reactors (Cacuci, 2010). Table 10 shows the summary of few important studies on core-degradation leading to severe accidents.

Hagen and Hofmann (1987) conducted an out-of-pile experiments on zircaloy clad-UO_2 fuel assembly at a temperature of 2200 °C under oxidizing environment. The following was the outcome of their study:

- The chemical interaction between zircaloy clad and UO_2 fuel occurred at the same rate as the steam zircaloy reaction. The embrittlement was found four times faster than oxidation from either surface alone.
- The dissolution of UO_2 by molten zircaloy resulted in a drastic increase in volatile fission products. The dissolution had been

Table 10
Studies on core degradation phenomena.

Author (year)	Aspect	Remarks
Hagen and Hofmann (1987)	Severe accidents effect on clad-UO_2 assembly	Inside clad surface oxidation occurred due to UO_2 at high temperature
Hofmann (1999)	Core degradation	Contribution towards clad embrittlement due to oxygen uptake was found to be of same nature for both surface oxidations
Duijvestijn and Birchley (1999)	Core melt down and vessel failure	In absence of heat removal and no effective external cooling, major core degradation caused the vessel failure after 1–5 h
Lewis et al. (2009)	Severe fuel deformation behavior	Melting of Ag–In–Cd absorber alloys started at 1073 K and with increase in temperature finally leads to melting of UO_2 at 3120 K

described by a parabolic rate law, which was found to have an Arrhenius dependence on temperature.
- The failure temperature of (Ag–In–Cd) absorber rods was influenced by the guide-tube material. The absorber rod failed at 1200 °C.

Hofmann (1999) reviewed the core degradation phenomena in reactors. The author divided the core-degradation phenomena in two phases: early-phase of core degradation and the late-phase of core degradation. It was pointed out that the former phase had been extensively studied whereas latter had not much discussed. It was found that the late-phase degradation played a vital role in plant safety studies such as in areas like hydrogen generation, release of fission products and wall vessel attack.

The study on core meltdown along with vessel failure was performed by Duijvestijn and Birchley (1999). They worked mainly on the late-phase core melting of PWR leading to the vessel failure. It was found that:

- The core debris characteristics and thermodynamic conditions affected the failure time period. Presence of metallic component within oxide fuel debris accelerated the failure process of vessel.
- Vessel failure took place after 1–5 h of start of major core degradation.

A recent study on severe fuel deformation as result of core degradation has been done by Lewis et al. (2009). The temperature dependent stage-wise core degradation leading final reactor meltdown has been studied. As a first stage, the melting of Ag–In–Cd absorber at 1073 K takes place, which is followed by the clad burst in a temperature range of 1020–1370 K depending on the system pressure. Further deterioration of zircaloy clad due to severe oxidation leads to melting of zircaloy at 2030 K, which is subsequently followed by the partial melting of UO_2. The complete core meltdown occurs at 3120 K.

4. Concluding remarks

Almost every aspect of the clad tube failure has been covered in the present review. The important points have been highlighted under different headings. Following conclusions can be drawn:

1. Zircaloy-2 and zircaloy-4 have been in used as clad materials from past 50 years. With the development in high burnup fuels, zircaloy-2 and zircaloy-4 are not suitable for these applications. ZIRLO and M5 are being used in reactors where high burnup fuels are used as they have good creep strength at higher temperature. Not to limit the scope of future development in clad tube material, improved ZIRLO known as OPT ZIRLO has been developed but is yet to commercialize. Another newer clad material which has been developed and not yet commercialized is X5A. This material has lower hydrogen pickup as compared to ZIRLO and has lower fuel rod growth.
2. During LOCA, the corrosion rate and creep rate increases significantly.
   a. During corrosion, three layers are formed on the clad surface. The outermost is brittle ZrO_2 scale, the middle layer is brittle oxygen rich α-layer and the innermost layer is β-layer is only load bearing layer. The thinning of this layer would endanger the structural integrity. Further, the hydrogen absorption in this layer also makes it brittle.
   b. During creep or plastic deformation, anisotropy in HCP α-phase causes clad tube ballooning and its subsequent shortening. There is a rise in circumferential burst strain with burst temperature in α-phase and a fall in β-phase. In the mixed phase, the circumferential burst strain first decreases and then increases. This reversal of strain behavior in the β-phase is attributed to the influence of oxidation of zircaloy.
   c. The effect outside medium on the corrosion and creep has a role to play. It has been seen that air medium is not an adequate medium to study oxidation. The air grown scales do not exhibit load bearing capability. Steam environment, on the other hand, causes an oxidation on clad surface which is governed by Arrhenius equation. There is no effect of steam and inert atmosphere on the strain rate. However, the strain rate is more in vacuum environment as compared to that in steam environment.
3. During RIA, the increased reactivity may cause the fuel pellets with in clad to deform. The clad tube after coming in contact with the deformed pellet takes it shape and the cracks develop. The interaction of fuel pellet with the clad (PCMI) has been found to occur in between 200 W/cm and 500 W/cm. DNB occurs due to the formation of non-conducting vapour layer on the clad outer surface, which results in an increase in clad surface temperature. It can be avoided by increasing the pressure or mass flow rate of the coolant.
4. The criterion for equivalent cladding reacted (ECR) is 15% in Japan and 17% in USA.
5. The core-degradation phenomena have been suggested to occur in two phases: early-phase of core degradation and the late-phase of core degradation. The early phase has been extensively studied whereas the late phase has gained a little attention despite of its vital role in plant safety studies.

Acknowledgments

We express our sincere acknowledgment to the Atomic Energy Regulatory Board (AERB), Government of India, for financing the ongoing research project on zircaloy clad failure.

References

Arai, S., Murabayashi, H., Tanabe, A., Yoshida, K., Sumida, S., 1987. Failure correlation for zircaloy-2 fuel cladding under high temperature transient conditions. Journal of Nuclear Science and Technology 24 ((March) 2), 214–219.
Aronson, S., 1960. Some Experiments on the Permeation of Hydrogen through Oxide Films on Zirconium, U.S. Report, Bettis Technical Review, WAPD-BT-19, June, pp. 75–81.
Asmolov, V., Yegorova, L., Lioutov, L., Konobeyev, K., Smirnov, A., Goryachev, V., Chesanov, A., Prokhorov, V., 2002. Understanding LOCA-related ductility in E110 cladding. In: Proc. Nuclear Safety Research Conference, October 28–30, 2002, Washington, DC.

Austin, J.H., Elleman, T.S., Verghese, K., 1974. Tritium diffusion in zircaloy-2 in the temperature range – 78–204 °C. Journal of Nuclear Materials 51, 321.
Azevedo, C.R.F, 2011. Selection of fuel cladding material for nuclear fission reactors. Engineering Failure Analysis, doi:10.1016/j.engfailanal.2011.06.010, Table 8.
Bauer, A., Lowry, L.M., Gallaghar, W.J.,1979. Tube-burst response of irradiated zircaloy spent fuel cladding. In: Zirconium in the Nuclear Industry (Fourth Conference), ASTM-STP 681. American Society for Testing and Materials, pp. 465–476.
Burman, D.L., Davis, D.D., Hochreiter, L.E., Lutz, R.D.,1984. Fuel rod deformation in LOCA and severe core damage accidents. In: ASTM-STP 824. American Society for Testing and Materials, pp. 780–792.
Cacuci, D.G., 2010. Handbook of Nuclear Engineering, Volume 1, Nuclear Engineering Fundamentals. Springer.
Cathcart, J.V., Pawel, R.E., McKee, R.A., Druschel, R.E., Yurek, G.J., Campbell, J.J., Jury, S.H., 1977. Zirconium Metal-Water Oxidation Kinetics, W. reaction rate Studies, Tech. Rep. ORNL/NUREG-17. Oak Ridge National Laboratory.
Chapman, R.H., Crowley, J.L., Longest, A.W., Hofmann, G.,1979. Zirconium cladding deformation in a steam environment with transient heating. In: ASTM-STP 681. American Society for Testing and Materials, pp. 393–408.
Chung, H.M., 2005. Fuel behavior under loss-of-coolant accident situations. Nuclear Engineering and Technology 37 ((August) 4).
Chung, H.M., Garde, A.M., Kassner, T.F., 1977. In: Lowe Jr., A.L., Parry, G.W. (Eds.), Rupture Behaviour of Zircaloy Cladding Under Simulated Loss-of-Coolant Accident Conditions, Zirconium in the Nuclear Industry, ASTM STP 633. American Society for Testing and Materials, pp. 82–97.
Coleman, E.,2002. Simulating the behavior of zirconium-alloy components in nuclear reactors. In: ASTM-STP 1423. American Society for Testing and Materials, pp. 3–19.
Cox, B., Roy, C., 1965. The Use of Tritium as a Tracer in Studies of Hydrogen Uptake by Zirconium Alloys, Atomic Energy of Canada Ltd., Report AECL-2519, December.
Cox, B., 1985. Mechanisms of Hydrogen Absorption by Zirconium Alloys, Atomic Energy of Canada Ltd., Report No. AECL-8702.
Cox, B., 2005. Some thoughts on the mechanisms of in-reactor corrosion of zirconium alloys. Journal of Nuclear Materials 336, 331–368.
Duijvestijn, G., Birchley, J., 1999. Core meltdown and vessel failure: a coupled problem. Nuclear Engineering and Design 191, 17–30.
Dupin, N., Ansara, I., Servant, C., Toffolon, C., Lemaignan, C., Brachet, J.C., 1999. A thermodynamic database for zirconium alloys. Journal of Nuclear Materials 275, 287–295.
Elbachiri, K., Doumalin, P., Crepin, J., Bornert, M., Barberis, P., Rebeyrolle, V., Bretheau, T., 2008. Characterization of local strain distribution in zircaloy-4 and M5 alloys. Journal of ASTM International 5 (9).
Elmoselhi, M.B., Warr, B.D., McIntyre, S.,1994. Study of the hydrogen uptake mechanism in zirconium alloys. In: ASTM-STP 1245. American Society for Testing and Materials, pp. 62–79.
Emmerich, K.M., Juenke, E.F., White, J.F.,1969. Failure of pressurized zircaloy tubes during thermal excursions in steam and in inert atmospheres. In: ASTM-STP 458. American Society of Testing Materials, pp. 252–268.
Erbacher, F., Neitzel, H.J., Weihr, K.,1979. Studies on zircaloy fuel clad ballooning in a loss-of-coolant accident-results of burst tests with indirectly heated fuel rod simulators. In: ASTM-STP 681. American Society for Testing and Materials, pp. 429–446.
Erbacher, F.J., Neitzel, H.J., Rosinger, H., Schmidt, H., Weihr, K.,1982. Burst criterion of zircaloy fuel claddings in a loss-of-coolant accident. In: ASTM-STP 754. American Society for Testing and Materials, pp. 271–283.
Erbacher, F.J., Leistikow, S.,1987. Zircaloy fuel cladding behavior in a loss-of-coolant accident: a review. In: ASTM-STP 939. American Society for Testing and Materials, pp. 451–488.
Ferner, J., Rosinger, H.E., 1985. The effect of circumferential temperature variation on fuel cladding failure. Journal of Nuclear Materials 132, 167–172.
Fiveland, W.A., Barber, A.R., Lowe Jr., A.L.,1977. Rupture characteristics of zircaloy-4 cladding with internal and external simulation of reactor heating, zirconium in the nuclear industry. In: ASTM-STP 633. American Society for Testing and Materials, pp. 36–49.
Foster, J.P., Yueh, H.K., Comstock, R.J., 2008. ZIRLO cladding improvement. Journal of ASTM International 5 (7).
Furuta, T., Kawasaki, S., Hashimoto, M., 1978. Zircaloy-clad fuel rod burst behavior under simulated loss-of-coolant condition in pressurized water reactors. Journal of nuclear Science and Technology 15 ((October) 10), 736–744.
Furuta, T., Motohashi, H., 1980. Products at the surface of zircaloy cladding under LOCA conditions. Journal of Nuclear Materials 95, 30–306.
Furuta, T., Uetsuka, H., Kawasaki, S.,1984. Estimation of conservatism of present embrittlement criteria for zircaloy fuel cladding under LOCA. In: ASTM-STP 824. American Society for Testing and Materials, pp. 734–746.
Garde, A.M., Comstock, R.J., Pan, G., Baranwal, R., Hallstadius, L., Cook, T., Carrera, F., 2010. Advanced zirconium alloy for PWR applications. Journal of ASTM International 7 (9).
Garzarolli, F., Stehle, H., Steinberg, E.,1996. Behavior and properties of zircaloys in power reactors: a short review of pertinent aspects in LWR fuel. In: ASTM-STP 1295. American Society for Testing and Materials, pp. 12–32.
Gilbert, E.R., Duran, S.A., Bement, A.L.,1969. Creep of zirconium from 50 to 850 °C. In: ASTM-STP 458. American Society of Testing Materials, pp. 210–225.
Gulbransen, E.A., Andrew, K.E., Dec. 1957. Reaction of hydrogen with preoxidized zircaloy-2 at 300 to 400 °C. Journal of Electrochemical Society Vol. 104 (12).
Hagen, S., Hofmann, P., 1987. LWR fuel rod behavior during severe accidents. Nuclear Engineering and Design 103, 85–106.
Hannerz, K., Vesterlund, G., 1975. Zircaloy cladding mechanical properties. Nuclear Engineering and Design 33, 205–218.
Hardy, D.G., Stewart, J.R., Lowe Jr., A.L.,1974. Development of a closed-end burst test procedure for zircaloy tubing. In: ASTM-STP 551. American Society of Testing Materials, pp. 14–30.
Hill, R., 1948. A theory of yielding and plastic flow of anisotropic metals. Proceeding of Royal Society 193, 281–297.
Hindle, E.D., Mann, C.A.,1982. An experimental study of the deformation of zircaloy PWR fuel rod cladding under mainly convective cooling. In: ASTM-STP 754. American Society for Testing and Materials, pp. 284–302.
Hofmann, P., Neitzel, H.J.,1987. Experimental and theoretical results of cladding oxidation under severe fuel-damage conditions. In: ASTM-STP 939. American Society for Testing and Materials, pp. 504–538.
Hofmann, P., 1999. Current knowledge on core degradation phenomena, a review. Journal of Nuclear Materials 270, 194–211.
Hong, S.I., Kim, H.J., 1987. Temperature dependence of elongation in zircaloy-4. Material Science and Engineering 86, L1–L4.
Hong, S.I., Ryu, W.S., Rim, C.S., 1983. Elongation minimum and strain rate sensitivity minimum of zircaloy-4. Journal of Nuclear Materials 116, 314–316.
Jacques, P., Lefebvre, F., Lemaignan, C., 1999. Deformation–corrosion interactions for Zr alloys during I-SCC crack initiation part I: chemical contributions. Journal of Nuclear Materials 264, 239–248.
Kaddour, D., Frechinet, S., Gorgues, A.F., Brachet, J.C., Portier, L., Pineau, A., 2004. Experimental determination of creep properties of zirconium alloys together with phase transformation. Scripta Materials 51, 515–519.
Kass, S.,1964. The development of the zircaloys. In: American Society of Testing Materials ASTM-STP 368. American Society for Testing and Materials, EB/NOV.
Kim, J.H., Lee, M.H., Choi, B.K., Jeong, Y.H., 2004. Deformation of zircaloy-4 cladding during a LOCA transient up to 1200 °C. Nuclear Engineering and Design 234, 157–164.
Kim, J.H., Choi, B.K., Baek, J.H., Jeong, Y.H., 2006. Effects of oxide and hydrogen on the behavior of zircaloy-4 cladding during the loss of coolant accident (LOCA). Nuclear Engineering and Design 236, 2386–2393.
Krishnan, R., Asundi, M.K., 1981. Zirconium alloys in nuclear technology. Proceedings of the Indian Academy of Sciences (Engineering Science) 4 ((April) Pt. 1), 41–56.
Lewis, B.J., Iglesias, F.C., Dickson, R.S., Williams, A., 2009. Overview of high-temperature fuel behavior with relevance to CANDU fuel. Journal of Nuclear Materials 394, 67–86.
Lewis, B.J., Thompson, W.T., Kleczek, M.R., Shaheen, K., Juhas, M., Iglesias, F.C., 2011. Modelling of iodine-induced stress corrosion cracking in CANDU fuel. Journal of Nuclear Materials 408, 209–223.
Lee, S.Y., Kim, K.T., Hong, S.I., 2009. Circumferential creep properties of stress-relieved zircaloy-4 and Zr–Nb–Sn–Fe cladding tubes. Journal of Nuclear Materials 392, 63–69.
Lee, K.W., Kim, S.K., Kim, K.T., Hong, S.I., 2001. Ductility and strain rate sensitivity of zircaloy-4 nuclear fuel claddings. Journal of Nuclear Materials 295, 21–26.
Lustman, B.,1979. Zirconium technology – twenty years of evolution. In: ASTM-STP 681. American Society for Testing and Materials, pp. 5–18.
Maki, H., Ooyama, 1976. Behavior of zircaloy fuel cladding tubes. Journal of Nuclear Science and Technology 13 ((February) 2), 43–57.
Matthews, J.R., 1984. The effect of anisotropy on the ballooning of zircaloy cladding. Nuclear Engineering and Design 77, 87–95.
Mardon, J.-R., Charquet, D., Senevat, J.,2000. Influence of composition and fabrication process on out-of-pile and in-pile properties of M5 alloy. In: ASTM-STP 1354. American Society for Testing and Materials, pp. 505–524.
Mardon, J.P., Garner, G.L., Hoffmann, P.B., 2010. M5® a breakthrough in Zr alloy. In: 2010 LWR Fuel Performance Meeting/Top-Fuel/WRFPM, September 26–29, 2010, Orlando, FL, USA.
Mishima, Y., Aoki, T., Ito, G., Kiyooka, S., Ono, K., Seki, Y., Sumitomo, M., Takao, Z., 1966. Behavior of cladding tube under coolant-loss-accident conditions. Journal of Nuclear Science and Technology 3 ((February) 2), 72–82.
Nagase, F., Chuto, T., Fuketa, T., 2009. Behavior of high burn-up fuel cladding under LOCA conditions. Journal of Nuclear Science and Technology 46 (7), 763–769.
NEA, 2010a. Nuclear Fuel Behaviour under Loss-of-Coolant Accident (LOCA) Conditions. Organization for Economic Cooperation and Development, Nuclear Energy Agency, NEA No. 6846.
NEA, 2010b. Nuclear Fuel behaviour in Reactivity-initiated Accident (RIA) Conditions. Organization for Economic Cooperation and Development, Nuclear Energy Agency, NEA No. 6847.
Nikulina, A.V., 2004. Zirconium alloys in nuclear power engineering. Material Science and Heat Treatment 46 (11–12), 458–462.
Picklesimer, M.L., 1987. Anisotropy in Zircaloy, ASTM-STP 939. American Society of Testing Materials (ASTM), Philadelphia, pp. 23–34.
Pickman, D.O., 1972. Properties of zircaloy cladding. Nuclear Engineering and Design 21, 212–236.
Pickman, D.O.,1994. Zirconium alloy performance in light water reactors: a review of UK and Scandinavian experience. In: ASTM-STP 1245. American Society for Testing and Materials, pp. 19–32.
Rosinger, H.E., Bera, P.C., Clending, W.R., 1979. Steady-state creep of zircaloy-4 fuel cladding from 940–1873 K. Journal of Nuclear Materials 82, 286–297.
Rosinger, H.E., 1984. A model to predict the failure of zircaloy-4 fuel sheathing during postulated LOCA conditions. Journal of Nuclear Materials 120, 41–54.
Roy, C., 1964. Hydrogen Distribution in Oxidized Zirconium Alloys by Autoradiography, Atomic Energy of Canada Ltd. (AECL), Report No. AECL-2085, September.

Sabol, G.P., Kilp, G.R., Balfour, M.G., Roberts, E.,1989. Development of a cladding alloy for high burn up. In: ASTM-STP 1023. American Society for Testing and Materials, pp. 227–244.

Sabol, G.P., 2005. ZIRLO – an alloy development success. Journal of ASTM International 2 ((February) 2).

Sagat, S., Sills, H.E., Walsworth, J.A.,1984. Deformation and failure of zircaloy fuel sheaths under LOCA conditions. In: ASTM-STP 824. American Society for Testing and Materials, pp. 709–733.

Saux, M. Le., Besson, J., Carassou, S., Poussard, C., Averty, X., 2009. Behavior and failure of uniformly hydride zircaloy-4 claddings between 25 °C and 480 °C under various stress states, including RIA loading conditions. Engineering Failure Analysis, doi:10.1016/j.engfailanal.2009.07.001.

Sawatzky, A.,1979. A proposed criterion for the oxygen embrittlement of zircaloy-4 fuel cladding. In: Zirconium in the Nuclear Industry (Fourth Conference), ASTM STP 681. American Society for Testing and Materials, pp. 479–496.

Seok, M.B., Srikant, G., Murty, K.L., 2007. High Temperature Deformation Characteristics of ZIRLO Tubing via Ring Creep and Burst Test, Transactions, SMiRT 19, Toronto, August.

Shannon, D.W., 1963. Effect of oxidation rates on hydriding of zirconium alloys in gas mixtures containing Hydrogen. Corrosion 19 (December), 414–420.

Shimada, S., Cheng, B., Lutz, D., Kubota, O., Ichikawa, N., Ibe, H., 2005. In-core tests of effects of BWR water chemistry impurities on zircaloy corrosion. Journal of ASTM International 2 (5).

Sidky, P.S., 1998. Iodine stress corrosion cracking of zircaloy reactor cladding: iodine chemistry (a review). Journal of Nuclear Materials 256, 1–17.

Sills, H.E., Holt, R.A.,1979. Predicting high temperature transient deformation from microstructural models. In: ASTM-STP 681. American Society for Testing and Materials, pp. 325–341.

Smith, T., 1965. Diffusion coefficients and anion vacancy concentration for the zirconium–zirconium dioxide system. Journal Electrochemical Society (June), 560–567.

Steinbrück, M., Böttcher, M., 2011. Air oxidation of zircaloy-4, M5® and ZIRLO™ cladding alloys at high temperatures. Journal of Nuclear Materials, doi:10.1016/j.jnucmat.2011.04.012.

Stern, A., Brachet, J.-C., Malliot, V., Hamon, D., Barcelo, F., Poissonnet, S., Pineau, A., Mardon, J.-P., Lesbros, A., 2008. Investigation of the microstructure and mechanical properties of prior-β structure as a function of the oxygen content in two zirconium alloys. Journal of ASTM International 5 (4).

Steinar, A.A.S., 1972. Mechanical interaction between fuel and cladding. Nuclear Engineering and Design 21, 237–253.

Teichel, H., Pouget-Abadie, X., 1999. How the European pressurised water reactor fulfils the utility requirements. Nuclear Engineering and Design 187, 9–13.

Tobais, A., 1980. Decay heat. Progress in Nuclear Engineering 5 (1), 1–93.

Uetsuka, H., Furuta, T., Kawasaki, S., 1983. Failure-bearing capability of oxidized zircaloy-4 cladding under simulated loss of coolant condition. Journal of Nuclear Science and Technology 20 ((November) 11), 941–950.

Uetsuka, H., Furuta, T., Kawasaki, S., 1982. Embrittlement of zircaloy-4 due to oxidation in environment of stagnant steam. Journal of Nuclear Science and Technology 19 ((February) 2), 158–165.

Woolsey, I.S., Morris, J.R., 1981. A study of zircaloy-2 corrosion in high temperature water using ion beam methods. Corrosion 37, 575–585.

Wart, B.D., Elmoselhi, M.B., McIntyre, N.S., Brennenstuhl, A.B., Lichtenberger, P.C., Newcomb, S.B., 1991. Oxide characteristics and their relationship to hydrogen uptake in zirconium alloys. In: ASTM-STP 1132, Philadelphia. American Society for Testing and Materials, pp. 740–757.

Yamanaka, S., Higuchi, K., Miyake, M., 1995. Hydrogen solubility in zirconium alloys. Journal of Alloys and Compounds 231, 503–507.

Yamanaka, S., Miyake, M., Katsura, M., 1997. Study on the hydrogen solubility in zirconium alloys. Journal of Nuclear Materials 247, 315–321.

Zhou, Y., Devarajan, B., Murty, K.L., 2004. Short term rupture studies of zircaloy-4 tubing using closed-end internal pressurization. Nuclear Engineering and Design 228, 3–13.